OFFICE OF NAVAL RESEARCH

Contract #N7 ONR 421 I

Project Designation #NR 330-004

Our Case Number C47736

Technical Report No. 7

FACTORS AFFECTING THE TRANSLATION OF CERTAIN MECHANICAL PROPERTIES OF CORDAGE FIBERS AND YARNS INTO CORDAGE STRANDS AND ROPES

by

M. M. Platt, W. G. Klein, and W. J. Hamburger

Fabric Research Laboratories, Inc.
665 Boylston Street
Boston, Massachusetts

1 December, 1953

SUMMARY

This report is concerned with the quantitative analysis of some of the factors which determine the strength of cordage strands and plied yarns. When integrated with the analyses covered in Technical Report Number 6 on this project, a complete picture is given of the effects of the factors considered on translation of the strength of cordage fibers into singles yarns, strands or plied yarns and, by direct projection, into cordage ropes. The problem is solved by a combined mechanical-statistical analysis similar in type to that given in Technical Report Number 6, assuming simplified idealized geometrical forms and a normal distribution of yarn properties. It is shown that such assumptions produce results which agree, within the limits of engineering accuracy, with experimental results. Experimental checks were available for: 9 rope strands of varying twist structure, all made of Manila abaca fiber; a small Sansevieria three-ply rope; and small size bundles of Manila abaca fiber used as laboratory models to illustrate the effect of number of singles in a strand or plied yarn.

The factors which are mathematically analyzed for their mechanical effects include: singles yarn twist; strand or plied yarn twist; number of singles which are stranded; elastic properties of the singles yarns; and uniformity of the mechanical properties of the singles yarns.

For the strand and rope structures studied, translational efficiencies of fiber strength of the order of 40% were observed. It is shown that significant losses occur in the translation of the strength of the yarns into the strands and ropes, efficiencies of the order of 75% being theoretically calculated and experimentally verified. However, the major cause of the low overall 40% efficiencies of translation of fiber strength to strands and ropes resides in the low fiber to yarn translation of only 55%. The losses from yarns to strands are indicated to be the results of both low uniformity of yarn elongation to break and also the inclination of yarns to the strand and rope axes, both effects being equal in magnitude for most of the structures studied. Such equivalence, of course, would not necessarily exist in other structures. The coefficients of variation of yarn rupture elongation of about 10% for the yarns examined in this work appear, on the basis of the inherent variability of 20-30% for their constituent fiber to be the result of nonuniformities created by processing. Such levels of yarn nonuniformity do not lend themselves, at present, to significant reduction by alterations of manufacturing techniques, and thus it appears that improvements in yarn to strand or plied yarn translational efficiencies can only be practically accomplished by strand and rope twist reductions or by the use of more extensible fibers and yarns.

Aspects of the simplified geometric analyses are checked by comparing the results with the results of a more precise geometrical analysis of plied structures as developed by Chow (5). The differences between the results of the two approaches are shown to be negligible for the practical range of twisted structures, hence justifying the assumptions leading to the simplified analyses.

SUMMARY (continuation)

The results are presented in a graphical manner over a range of the variables far in excess of those commonly found and presently used in cordage structures. This is consistent with the long-range philosophy of the research, which is aimed at assessment of fibers not presently used in cordage structures. The graphically presented results are immediately applicable to the engineering calculations of the strength both of many cordage structures, and also other twisted structures such as tire cord and sewing thread. The limits of application are defined by the validity of the simplified geometric forms assumed.

TABLE OF CONTENTS

LIST OF TABLES

LIST OF FIGURES

LIST OF FIGURES (continuation)

INTRODUCTION

Previous work (1,2) has shown how the translation of strength from fiber to singles yarn of cordage type can be predicted with considerable accuracy from a combination of the effects of inherent fiber properties and yarn geometry. This report extends this work to higher order cordage structures such as strands, plied yarns, and ropes on the basis of a similar analysis. To effect such an analysis, a method has been developed for treating the statistically difficult range where the sampling is too small to utilize large approximations and yet large enough so that small sample methods are too cumbersome. Such intermediate sample sizes represent the case of plied yarns, strands, and ropes. The results are presented graphically in a manner which is immediately applicable with engineering accuracy to many cordage structures.

In Technical Report Number 6 on this project an analysis was made of the factors which affect the translation of fiber strength into singles yarns on the basis of inherent fiber properties and yarn geometry. The basic load equation derived in Technical Report Number 6 is:

$$P_y = 2\int_0^{R_y} \pi b\left(\frac{a}{b} + e_y \cos^2 \theta_y\right)\cos^2 \theta_y \frac{n_u}{100} r\, dr \quad \text{---------- (1)}$$

where P_y is the load supported by the yarn, a and b are constants found from the fiber stress-strain relationship, e_y is the yarn elongation corresponding to the yarn load P_y, θ_y is the helix angle at any point in the yarn cross section, n_u is the percent of fiber unbroken at an elongation $e_y \cos^2\theta_y$(3), and r is the radial distance from the yarn center. Important assumptions in the analysis leading to Equation (1) were: (a) the number of fibers in any element of yarn cross sectional area, $2\pi r dr$, is sufficiently large so that n_u may be defined uniquely and continuously as a function of both the strain in the fiber and the standard deviation of fiber rupture elongation, under the assumption of a normal distribution of fiber rupture elongation; (b) the fiber diameter was sufficiently smaller than the yarn diameter so that θ_y might be defined continuously as a function of r. Clearly, neither of these assumptions is valid for a plied yarn consisting of two or three or even seven singles yarns, where the singles yarn assumes the role of the fiber and the plied yarn that of the singles in the above expression. Nor is it obvious just how many units or what diameter ratios are necessary to make these assumptions valid. Thus, while the reasoning used to develop the above integral is valid, it must be replaced by a summation for the case of plied structures. In addition, since the plying operation may in general introduce excess lengths into the constituent singles yarns, the term $e_y\cos^2\theta$ in the load Equation (1) above is not necessarily the true strain on the fiber and must be modified to include crimp.

The following analysis is divided into four parts:

1.) The geometric effects of ply and yarn twist in various configurations on strength translation.

2.) The effects of yarn variability on strength translations.

3.) The combined effects of geometry and variability on strength translation and comparison with experiment.

4.) Examination of assumptions.

I. EFFECTS OF PLY TWIST

A. Determination of Ply Helix Angle

The axial load transmitted by a yarn inclined at an angle θ_p to the plied yarn axis is given by the expression:

$$P = P_y \cos \theta_p \qquad (2)$$

where P is the load parallel to the plied yarn axis and P_y is the load in the inclined yarn. Thus, each yarn in a plied yarn or strand contributes a supporting load equal to its own load times the cosine of its angle of inclination with the plied yarn axis. This angle of inclination of the yarn is taken to be that obtained from the expression (4):

$$\tan \theta_p = 2\pi N_p R_p \qquad (3)$$

where N_p is the turns per unit length of the plied yarn and R_p, the plied yarn helix radius, is the distance from the center of the plied yarn to the center of mass of the given singles yarn. It will be shown later, when the various assumptions are examined, that this definition leads to results that are in good agreement with the length - twist relationships that exist in the yarn of plied and stranded structures.

Three specific examples will illustrate the method of determining the angles of inclination, θ_p. By definition:

R_y = yarn radius

R_p = helix radius of plied yarn, the distance from the center of the plied yarn to the center of mass of the singles yarn in question.

θ_p = plied yarn helix angle, the angle between the axis of the singles yarn in question and the plied yarn axis.

Example 1: A two ply yarn, yarns of circular section (see Figure 1).

$R_p = R_y$

$\tan \theta_p = 2\pi N_p R_y$

Example 2: A three ply yarn, yarns of circular section (see Figure 2).

TWO PLY YARN

FIGURE 1

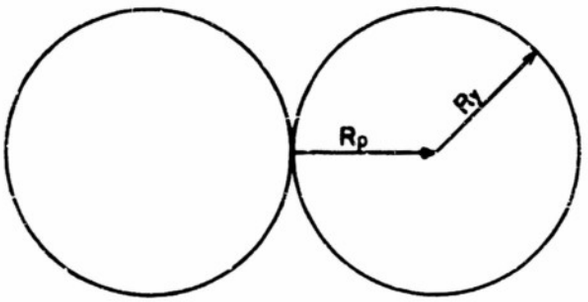

$$R_p = R_y$$

$$\theta_p = \arctan \; 2\pi N_p R_y$$

THREE PLY YARN

FIGURE 2

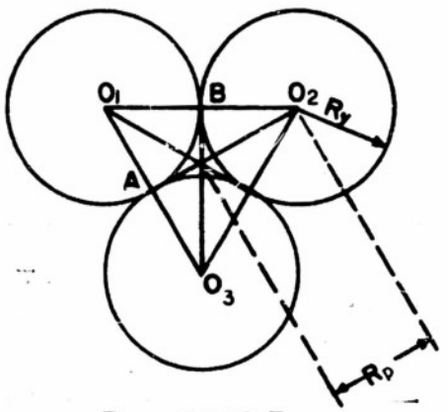

$$R_p = 1.155\, R_y$$

$$\theta_p = \arctan \; 2\pi N_p (1.155) R_y$$

FIFTEEN YARN STRAND

FIGURE 3

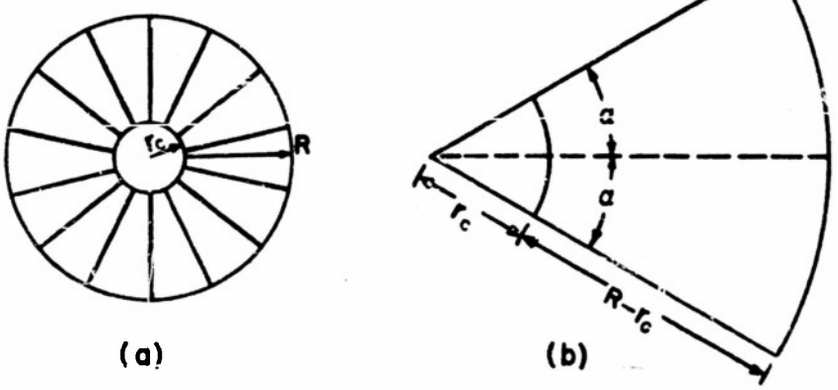

$$R_p = 0.694\, R$$

$$\theta_p = \arctan \; 2\pi N_p (0.694) R$$

$$R_p = \frac{2}{3}\sqrt{(2R_y)^2 - (R_y)^2} = 1.155R_y$$

$$\tan \theta_p = 2.310\pi N_p R_y$$

Example 3: A 15 yarn strand consisting of a single core yarn surrounded by 14 wedges (see Figure 3).

Since all 15 units are of about the same area, each has an area $\frac{\pi R^2}{15}$. For the circular core the area is πr_c^2 so that:

$$r_c^2 = \frac{R^2}{15}$$

and thus:

$$r_c = 0.258R$$

The core yarn obviously is inclined zero degrees to the strand axis. Now consider one of the yarns in the external ring. Its shape and dimensions are as shown in Figure (3b). For 14 units in the outer ring, the angle $\alpha = 12.85°$. By taking moments about the center of the strand, it can be shown that R_p, the distance between the center of the strand and the center of mass of each of the external yarns is:

$$R_p = 0.694R$$

and thus:

$$\tan \theta_p = 2\pi N_p(0.694)R$$

$$= 1.388\pi N_p R$$

Similar analyses can be made for any structure after the geometric configuration has been defined or approximated. Thus from the geometric configuration and the turns per unit length of the ply, an angle can be found whose cosine is the load transmission factor from singles yarn to plied yarn.

While this very simple relationship exists between plied yarn twist, helix radius, and load transmission there may, depending on processing, be two other important effects of ply twist. These are: a change in singles yarn helix angle; and an introduction of excess lengths into the yarns. These factors will now be investigated on the basis of two assumptions:

1.) The helix angle of the yarn as it lies in the ply can be determined from:

$$\tan \theta_{yp} = 2\pi N_{yp} R_y$$

where N_{yp} is the number of turns per unit length of the yarn as it lies in the ply. That is, the angles between fiber and yarn axes are not effected by the fact that the yarn axis is itself helical. As is shown later, this assumption introduces negligible errors into the results of the mechanical analysis.

2.) Excess fiber lengths are created by a reduction in yarn helix angle and can be expressed as the difference between the fiber path length required for the initial singles helix angle and the length required for the final singles helix angle.

B. Changes in Helix Angle of Singles Yarns due to Plying

The helix angle of a singlesyarn has been defined (3) as $\tan \theta_y = 2\pi N_y R_y$ where N_y is the turns per unit length of the singles yarn and R_y is the singles yarn radius. When a yarn is plied it is possible for the helix angles to be either increased, decreased, or unchanged, depending entirely upon the method of plying. In the case of pure twisting, that is, when the group of singles yarns can be considered to be clamped at both ends (see Figure 4a), twist can be considered to be inserted into the yarn or a turn for turn basis with ply twist. Whether this added twist is positive or negative depends upon whether the yarn and ply twists are in the same or the opposite sense (S on S, Z on Z, or S on Z, Z on S). The usual case is for twists in the opposite sense, so only this case will be considered. The total final equivalent twist in a yarn from a strand will then be $(N_{yo}-N_p)$ where N_{yo} is the total turns originally in a given length of singles yarn and N_p is the total turns in the corresponding length of ply. But since the length of a helical path is $\frac{\text{length of axis}}{\cos \theta}$, where θ is the helix angle, the singles yarn length is $\frac{\text{ply length}}{\cos \theta_p}$. Thus if N_p is the number of plied yarn turns per unit length of plied yarn axis, $\frac{N_p}{\frac{1}{\cos \theta_p}} = N_p \cos \theta_p$ turns per unit length of singles axis are subtracted from the yarn by plying and thus:

$$\tan \theta_{yp} = 2\pi (N_{yo} - N_p \cos \theta_p) R_y \qquad \text{---------- (4)}$$

where N_{yo} is the original turns per unit length of the singles yarn. If during the plying operation, a twist of N_{yl} turns per unit length of singles axis is added to the singles yarn, then $\tan \theta_y = 2\pi (N_{yo} - N_p \cos \theta_p + N_{yl})$ and the condition for perfect twist compensation, as shown in Figure (4b), should be:

$$N_{yl} = N_p \cos \theta_p \qquad \text{---------- (5)}$$

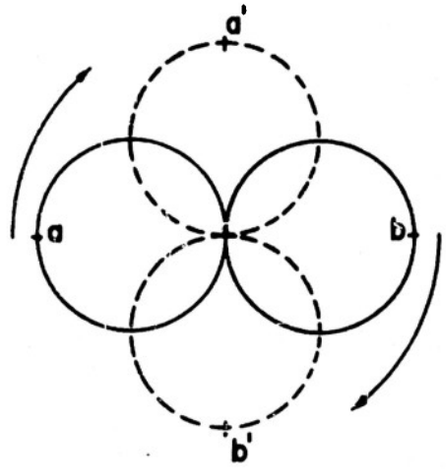

(a)
PURE TWISTING

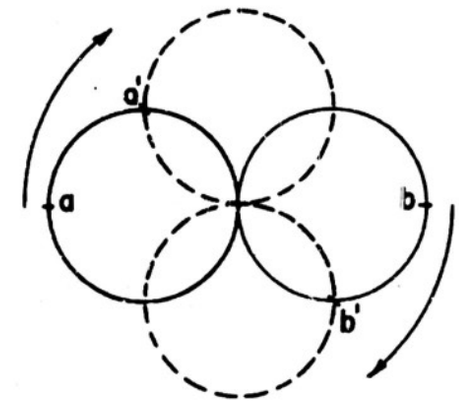

(b)
COMPLETE TWIST COMPENSATION

FIGURE 4

This relationship does not seem to hold precisely in practice although it is a good general guide. Discepancies are discussed in more detail later, as are the results of Chow's (5) more precise mathematical analysis of the geometry of plied yarns as it affects Equation 4 above.

C. Excess Lengths

If a singles yarn is partially untwisted by plying, the helix angle of any fiber in the yarn cross-section will decrease in a manner described by Equation 4 and consequently so will the required helical path length of each fiber. But unless then is opportunity for the excess lengths to be absorbed by a new geometric configuration, the final total length of any fiber in a given length of yarn untwisted by plying will be the same as it was before untwisting. The per cent difference between the original length of fiber and the length required for the new helical path, based on original length, will be called the excess length or crimp. Clearly the excess length will vary from zero at the center of a yarn, where untwisting has no angular effect, to a maximum at the outside of the yarn. The magnitude of these excess lengths in yarns of circular section will now be analyzed.

Consider a singles yarn with original external helix angle defined by $\tan \theta_{yo} = 2\pi N_{yo} R_y$, where N_{yo} is the original yarn twist and R_y the yarn radius. Then, the tangent of the helix angle at any radius r_y, is equal to $2\pi N_{yo} r_y$ with a corresponding helical path length per unit length of yarn:

$$\frac{1}{(\cos\theta_o)_r} = \sqrt{1 + (\tan^2\theta_o)_r} = \sqrt{1 + 4\pi^2 N_{y_o}^2 r_y^2} \quad \text{---------- (6)}$$

Now untwist the yarn until the number of turns per unit length is N_y. The required length of the helical path per unit length of yarn is now:

$$\sqrt{1 + 4\pi^2 N_y^2 r_y^2} \quad \text{---------- (7)}$$

and the per cent difference between the two lengths is:

$$\frac{\sqrt{1 + 4\pi^2 N_{yo}^2 r_y^2} - \sqrt{1 + 4\pi^2 N_y^2 r_y^2}}{\sqrt{1 + 4\pi^2 N_{yo}^2 r_y^2}} \times 100 \quad \text{---------- (8)}$$

Equation (8) defines the excess length, or the amount the fiber path must be extended before the fiber bears any appreciable tensile load, and thus must be included as a part of the fiber extension term in any expression for yarn load.

In deriving the expression given by Equation (1) for yarn load, e_f, the strain in a fiber, was taken as $e_y \cos^2\theta_y$ where e_y is the yarn strain and θ_y the helix angle for the given fiber. While $e_y \cos^2\theta_y$ still expresses the

total strain in the direction of the path, it does not define the part of the fiber strain which is load-bearing if any crimp is present. An expression for load-bearing fiber strain is derived as follows:

Let:

l_y = the singles yarn length

l_f = total fiber length in a length l_y of yarn = $\frac{l_y}{\cos \theta_{yo}}$

θ_{yo} = yarn helix angle before untwisting

θ_y = yarn helix angle after untwisting

Δl_y = yarn extension

Δl_f = total fiber path extension due to Δl_y.

$(\Delta l_f)_p$ = fiber path extension which is load-bearing.

e_y = yarn strain = $\frac{\Delta l_y}{l_y}$

$(e_f)_p$ = load-bearing fiber strain

From previous work (3):

$$\Delta l_f = \Delta l_y \cos \theta_y \qquad \text{(9)}$$

and, it is clear that:

$$(\Delta l_f)_p = \Delta l_f - l_y\left[\frac{1}{\cos \theta_{yo}} - \frac{1}{\cos \theta_y}\right] \qquad \text{(10)}$$

where the subtractive expression on the right side of Equation (10) represents the total crimp, or excess length created by the untwisting. Equation (10) assumes that the load required to straighten a crimped fiber is negligible compared to the load required to extend the same fiber in tension by an equal amount. Since:

$$(e_f)_p = \frac{(\Delta l_f)_p}{l_f} \qquad \text{(11)}$$

then, by combining (9), (10), and (11):

$$(e_f)_p = \frac{\Delta l_y \cos\theta_y - l_y\left[\frac{1}{\cos\theta_{yo}} - \frac{1}{\cos\theta_o}\right]}{\frac{l_y}{\cos\theta_{yo}}} \qquad \text{(12)}$$

which after simplification becomes:

$$(e_f)_p = e_y \cos\theta_y \cos\theta_{yo}\left[1 - \frac{\cos\theta_{yo}}{\cos\theta_y}\right] \qquad \text{(13)}$$

Noting that in the original expression for yarn load as a function of yarn strain, as given by Equation (1), the term $e_y\cos^2\theta_y$ represents the load-bearing fiber strain of a fiber, $(e_f)_p$, the above Equation (13) can be substituted for e_f, resulting in:

$$P_y = 2\pi\int_0^{R_y} b\left[\frac{a}{b} + e_y\cos^2\theta_{yo}\cos\theta_y - 1 + \frac{\cos\theta_{yo}}{\cos\theta_y}\right]\cos^2\theta_y \frac{n_u}{100}\, r\,dr \qquad \text{(14)}$$

or, in terms of r:

$$P_y = 2\pi\int_0^{R_y} b\left[\frac{a}{b} + e_y\left(\frac{1}{\sqrt{1+4\pi^2 N_{yo}^2 r^2}}\right)\left(\frac{1}{\sqrt{1+4\pi^2 N_y^2 r^2}}\right) - 1 + \frac{\sqrt{1+4\pi^2 N_y^2 r^2}}{\sqrt{1+4\pi^2 N_{yo}^2 r^2}}\right] \frac{1}{\left(1+4\pi^2 N_y^2 r^2\right)}\frac{n_u}{100}\, r\,dr$$

Reference to previous work (1,2) which gave general solutions for the maximum value of Py in terms of the several parameters when $N_y = N_{yo}$, will indicate the complexity of the problem when Nyo and Ny are not equal. Even assuming that an analytic solution could be found, an extremely large number of curves would be required to give any sort of generality to the work. Accordingly, no general solution was found. Instead, a piecewise summation was used to obtain approximate solutions for several specific cordage structures.

The procedure is as follows: Divide the yarn cross-section into five parts by inscribing four circles with radii $\frac{R_y}{5}$, $\frac{2R_y}{5}$, $\frac{3R_y}{5}$, and $\frac{4R_y}{5}$ and assume that each one of the rings so formed can be characterized by its properties at its midpoint (see Figure 5).

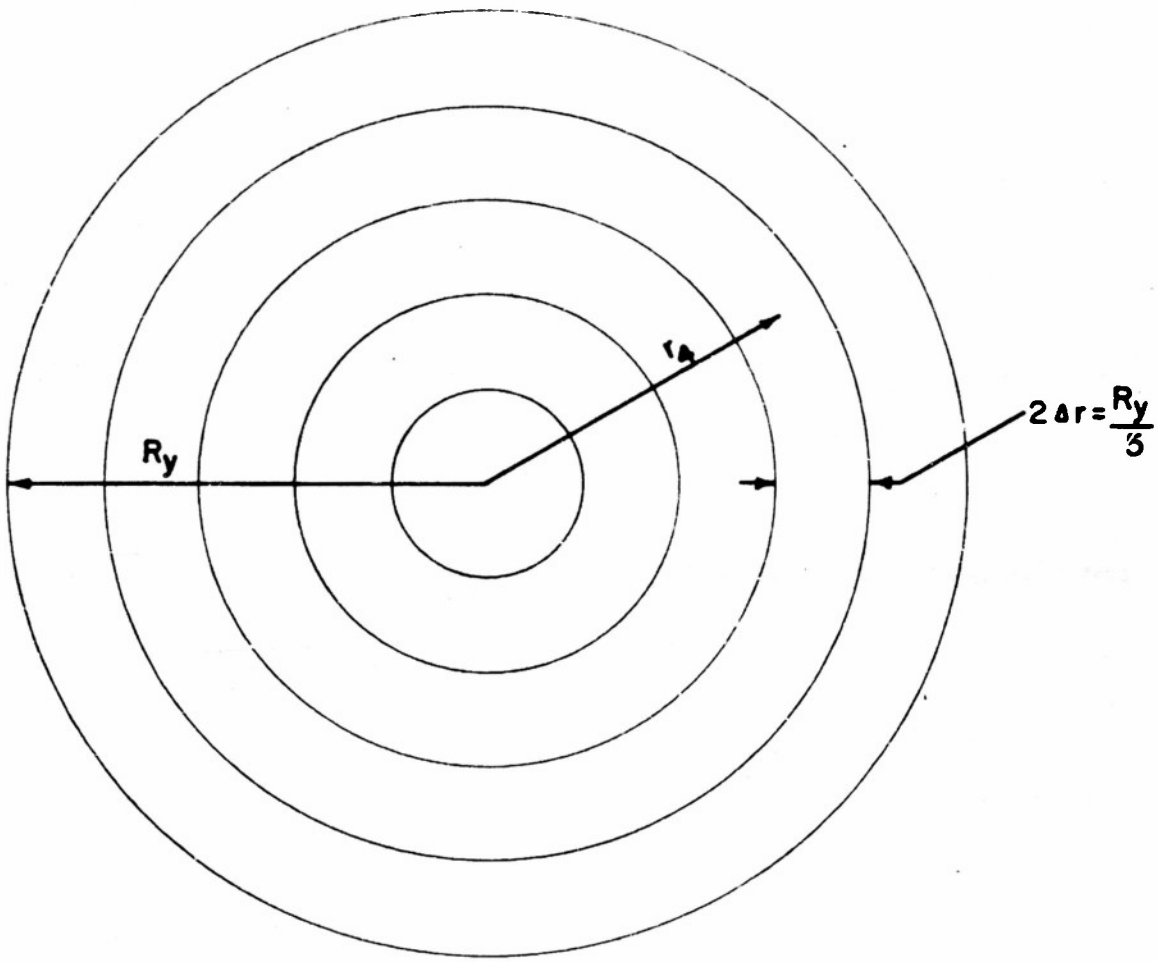

FIGURE 5

DIVISION OF YARN CROSS-SECTION FOR APPROXIMATE SOLUTION

Let:

p_i = Load per unit weight supported at midpoint of the ith ring.

e_i = Elongation of midpoint of the ith ring.

r_i = Radius to midpoint of the ith ring.

Δr = Half width of any ring.

θ_i = Helix angle at midpoint of the ith ring corresponding to the yarn twist, N_y

A_i = Area of ith ring.

$\bar{p}$ = Average strength per unit weight of fiber.

P_y = Total yarn load.

Since the weight is proportional to the area, the load in the ith ring will be:

$$P_i = Kp_iA_i$$

where K is a constant. Then the total load supported by all the rings will be:

$$P_y = \sum_{i=1}^{5} p_iA_i \cos^2\theta_i \frac{n_u}{100} \qquad \text{(15)}$$

This is entirely analogous to the expression:

$$P_y = 2\int_0^R \pi f \cos^2\theta_y \frac{n_u}{100} rdr$$

But:

$$A_i = \pi\left[(r_i + \Delta r)^2 - (r_i - \Delta r)^2\right] = 4\pi r_i \Delta r$$

and inspection of Figure (5) shows that $\Delta r = r_1$, so that:

$$A_i = 4\pi r_1 r_i$$

and thus:

$$P_y = 4\pi r_1 K \sum_{i=1}^{5} p_i r_i \cos^2\theta_i \frac{n_u}{100} \qquad \text{(16)}$$

If the structure were 100% efficient, the load would be $\bar{p}$, the mean fiber strength

per unit weight, times the total area, or:

$$\bar{K}\bar{p}\sum_{i=1}^{5} A_i \qquad \text{(17)}$$

Thus the per cent efficiency of translation of strength of the structure can be expressed as:

$$\eta = \frac{P_y(100)}{\bar{K}\bar{p}\sum_{i=1}^{5} A_i} = \frac{4\pi r_1 K \sum_{i=1}^{5} p_i r_i \cos^2\theta_i n_u}{\bar{p}\, 4\pi r_1 K \sum_{i=1}^{5} r_i} = \frac{\sum_{i=1}^{5} p_i r_i \cos^2\theta_i n_u}{\bar{p}\sum_{i=1}^{5} r_i} \qquad \text{(18)}$$

By assuming a given value of e_y, the corresponding value of η can be found as follows:

a.) Calculation of $(e_f)_p$ for each ring from Equation (13), utilizing the known geometry of the yarn to specify θ_{yo} and θ_y for each ring.

b.) The determination of appropriate value of P_i corresponding to $(e_f)_p$ for each ring from the fiber stress-strain curve.

c.) The calculation of n_u for each ring from $(e_f)_p$, the mean fiber rupture strain e_m, and the coefficient of variation of fiber rupture elongation V.

d.) The summation of Equation (18) for all rings.

By successively repeating this procedure for different values of e_y, a maximum η can be found.

The values of p_i must in general be found directly from the average fiber stress-strain curve, since with excess lengths the range of fiber strains for any given yarn strain is so great as to make the linear approximation used and described in Technical Report Number 6 too inaccurate.

The stress-strain curve used here differs slightly in type from that employed in previous work in which a plot of average grams per denier versus strain was used. The modification in the present work is to express the stress ordinate as average grams per average denier. Both types of curves for a given sample of Manila Abaca fiber are plotted in Figure(6). The fact that the curves formed by using the average grams per denier does not show the mean value of breaking stress occurring at the mean value of rupture elongation is a matter which required a modification factor in theoretical calculation of yarn efficiency as described in Technical Report Number 6.

The reason for using the curve of average grams per average denier rather than the average of the grams per denier will become clear after observing the formation of each of these quantities followed by comparison with the load expression in which they are used.

FIGURE 6

AVERAGE STRESS-STRAIN CURVES
MANILA ABACA FIBER

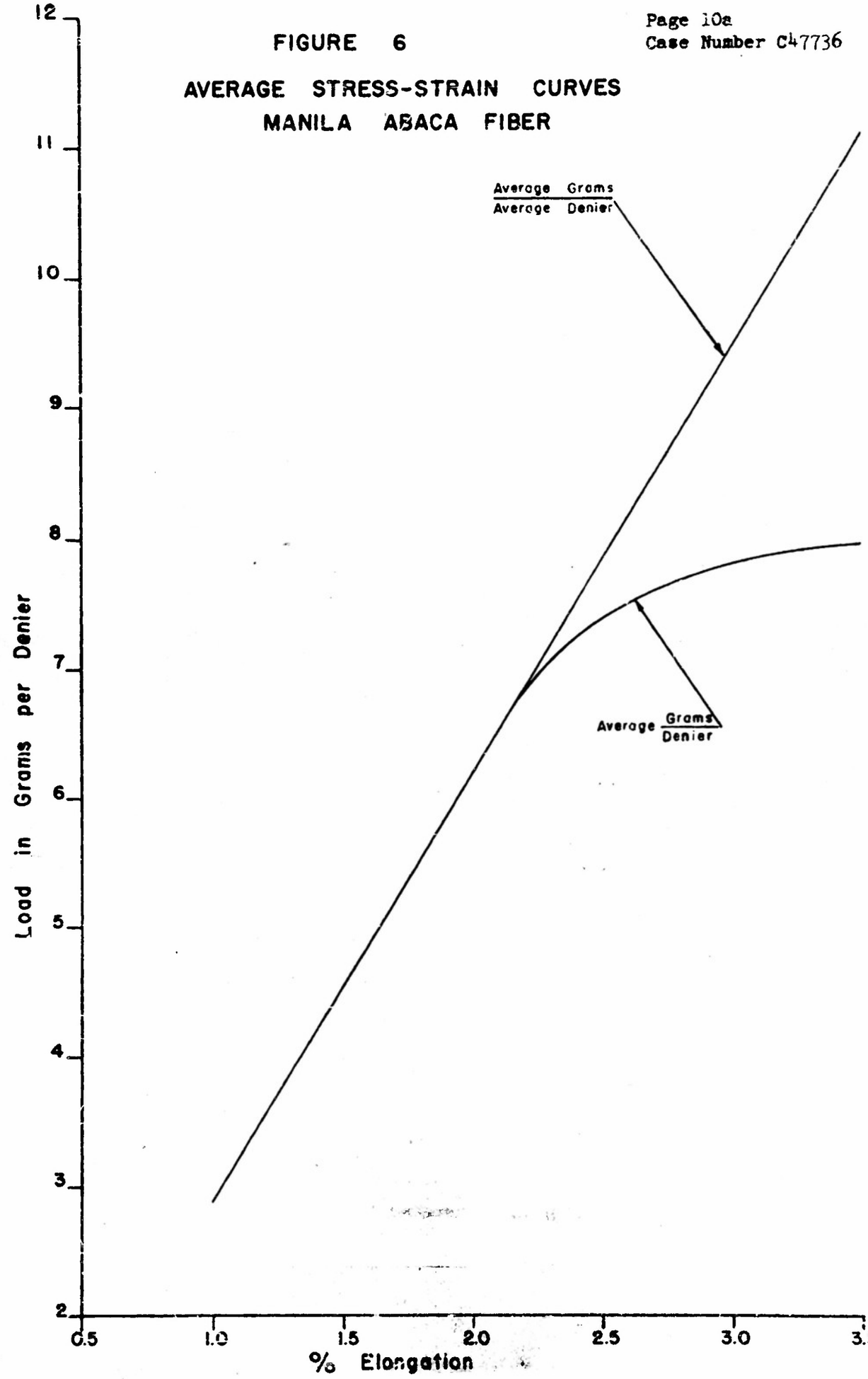

In forming a curve of average grams per denier versus strain, each fiber is weighed separately and the grams per denier of the fibers at given strains are averaged at enough different strains to delineate a curve. In plotting average grams per average denier, all fibers in the sample are weighed as a group, and the average load at various strains is divided by the average weight, in denier per fiber, of the whole original fiber sample to give the average grams per average denier. Expressed in analytic form, the procedure for finding the average grams per denier gives:

$$f(e) = \frac{\sum_{n(1-N_{fu})+1}^{n} \left(\frac{p_i}{w_i}\right)}{n(N_{fu})} \qquad (19)$$

while the average grams per average denier is determined from:

$$g(e) = \frac{\sum_{n(1-N_{fu})+1}^{n} \frac{p_i}{n(N_{fu})}}{\frac{W}{n}} = \frac{\sum_{n(1-N_{fu})+1}^{n} p_i}{W\,(N_{fu})} \qquad (20)$$

A simplification can be made to Equation (19) by realizing that when the values of $\frac{p_i}{w_i}$ are fairly symetrically distributed, the average value is very nearly $\frac{\sum p_i}{\sum w_i}$.

Therefore:

$$f(e) = \frac{\sum_{n(1-N_{fu})+1}^{n} \left(\frac{p_i}{w_i}\right)}{n(N_{fu})} = \frac{\sum_{n(1-N_{fu})+1}^{n} (p_i)}{\sum_{n(1-N_{fu})+1}^{n} (w_i)} \qquad (21)$$

What is desired is the total load supported by a bundle of fibers ($\sum p_i$) at any given elongation in terms of the stress-strain curve parameters. From Equation (21):

$$\sum p_i = f(e) \sum_{n(1-N_{fu})+1}^{n} (w_i)$$

and from Equation (20):

$$\sum p_i = g(e)\, W\left[N_{fu}(e)\right]$$

Thus to find $\sum p_i$ from the f(e) curve it is necessary to know $\sum_{n(1-N_{fu})+1}^{n} (w_i)$ or the total weight of the unbroken fibers at any given strain, while use of the g(e) curve requires only a knowledge of the total original weight of the bundle.

In the case where average fiber modulus is independent of tenacity, there would of course be no difference between the two Equations (20) and (21), but in the general case, such a dependence can be shown.

From Figure (6) it can be seen that the higher tenacity fibers have the lower modulus, or in other words that $\frac{\sum_{}^{n} (w_i)}{n(1-N_{fu}) + 1} > N_{fu} w.$

While results of previous calculations compensated with a correction factor for the "drooping" characteristic of curves defined by Equation (21), the most recent method is the more logical procedure in the sense that it properly expresses the load-carrying capacity of the aggregate structure. It offers the additional advantage that the average curve so defined has the same appearance as a single typical fiber stress-strain curve, while the former method introduces a distortion such that the average curve does not resemble any single given test curve. However, since experimental efficiencies are based on the mean breaking tenacity of the elements, it may, in some cases, be necessary to modify theoretical efficiencies obtained by use of the average grams per average denier curve so that they are consistent with the foregoing convention. This is conveniently done by multiplying theoretical efficiencies by the factor:

$$\frac{g(e_m)}{\text{mean rupture tenacity}}$$

where $g(e_m)$ is the ordinate to the average grams per average denier curve at mean rupture elongation. In general, it has been experimentally found that for cordage fibers and yarns the factor given above is extremely close to 1. Again, it is emphasized that the expression given above is not an arbitrary correction factor, but instead is necessary in order that theoretical and experimental efficiencies may be expressed on the same basis, namely, mean rupture tenacity.

Thus far a circular yarn cross-section has been assumed. For singles yarns, or yarns removed from strands, this seems to be a good approximation, but examination of strand sections shows that a yarn lying in the strand has a cross-section which may deviate considerably from the circular. An exact theoretical analysis of excess lengths for these distorted cases would be extremely complex geometrically but not particularly valuable practically because of the variety of shapes assumed by the yarns under different stranding conditions. Fortunately, the results are not so critically dependent on the exact shape of the yarn that certain rough approximations do not give satisfactory results. This aspect, together with deviations in results produced by differences in cross-sectional shapes, is covered in a subsequent section dealing with comparisons between theory and experimental results.

II. VARIABILITY

It was pointed out in the introduction that variability of elongation to break among singles yarns in a plied yarn cannot in general be treated in the same manner as variability among fibers in a yarn, and thus the magnitude of strength translation will be different for the two cases. A method is presented here the results of which make it possible to predict the effects of variability on the strength of small groups of fibers or yarns. The results also define the minimum size of the sample which gives essentially the same results as the large sample approximation developed and utilized in earlier work (1,2). The analysis applies equally to fibers, yarns, strands, or any elements which act as units in a large structure. For purposes of this analysis, a bundle of units is termed "parallel" if the geometry is such that all units are subjected to equal strains as a result of straining the group. Thus, two or three ply yarns of uniform geometry represent parallel bundles. The ply helix angle in this case necessitates the use of a geometric factor for efficiency calculations, which factor is independent of the statistical analysis which follows.

Suppose there exists a certain population of units and the results of many tensile tests of such units are plotted as a distribution of elongations to break. Then, if from the same population tensile tests of bundles of two units are made, consider the distribution of elongations to break of the first break in each group. Since the lowest elongation unit is the controlling factor, a high elongation unit paired with a low one would give no weight to the high one in the distribution. Similarly, it is clear that as the number of units in the bundle becomes larger, the average elongation at which the first unit breaks becomes lower. A method for obtaining the theoretical distributions of first unit breaks for various bundle sizes has been derived on the basis of a normal population of units and is found in Appendix (II). These distributions are plotted in Figure (7). For present purposes, the only concern will be the mean value of each of these distributions, and accordingly a curve of mean elongation at which first unit break occurs versus bundle size has been plotted in Figure (8), with elongation generalized in terms of t, the number of standard deviations from the unit population mean.

A question now arises as to the utility of these mean elongation curves with respect to the strength of a bundle or plied structure. It is obvious that if a bundle of two units is loaded, the total load will seldom exceed that reached when the first one breaks, so it can be said with certainty that the mean load for the first break in each bundle will also be very nearly the mean maximum bundle load. For example, if bundles of two units were tested, the mean breaking tenacity for the bundles would for a linear average stress-strain curve be that corresponding to an elongation of $e_m - 0.5\sigma$ (see Figure 8) on the average stress-strain curve for the population, when e_m is the mean breaking elongation for the population and σ is the population standard deviation of elongation to break. For the general case of non-linear stress-strain

FIGURE 7
DISTRIBUTION OF 1st UNIT RUPTURE
IN A BUNDLE vs BUNDLE ELONGATION

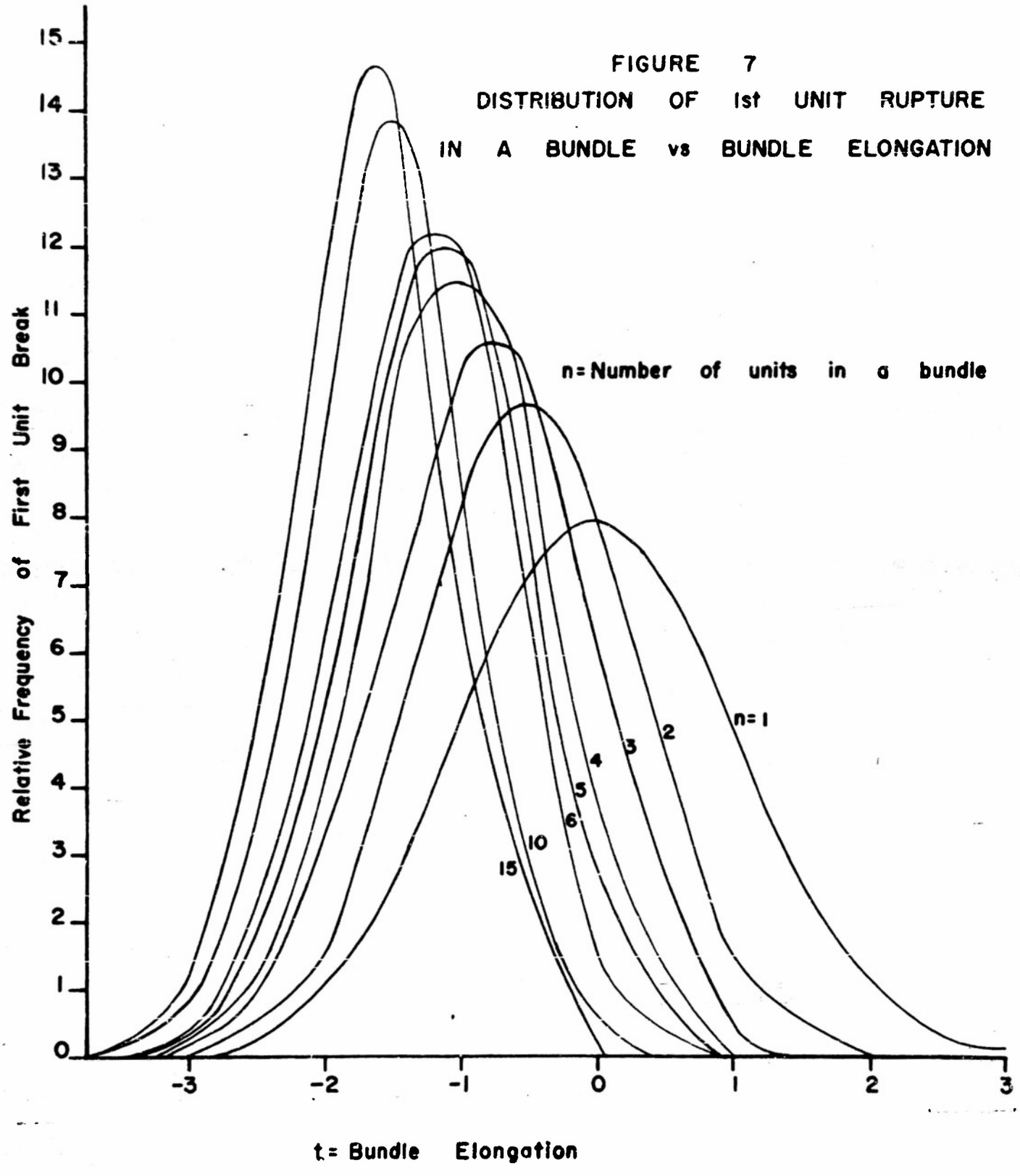

FIGURE 8

MEAN VALUE of t vs BUNDLE SIZE
FIRST UNIT BREAK

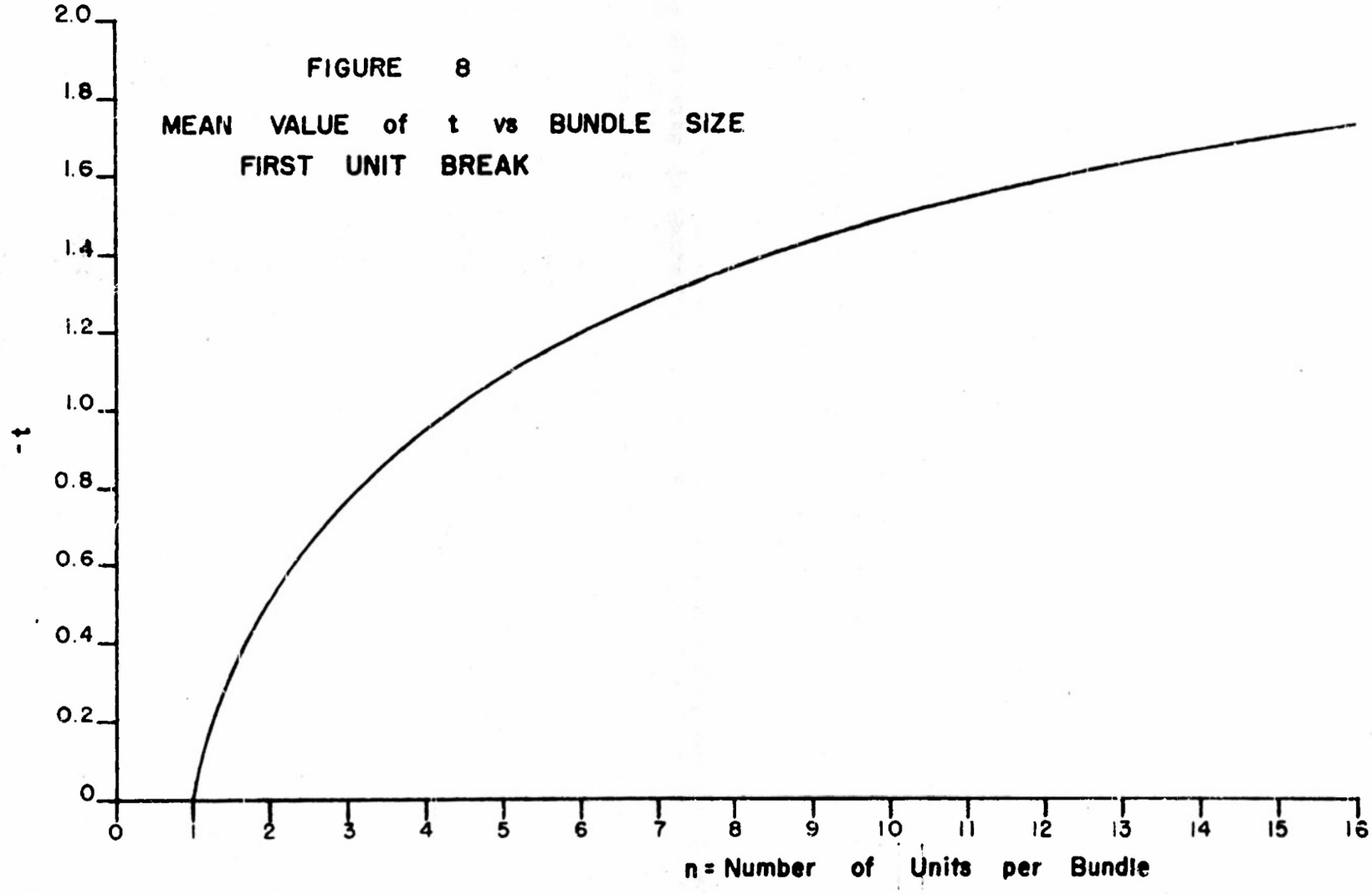

curves, it would be necessary to find the mean of the distribution curves of Figure (7) with the abscissa scale, t, converted to stress in order to obtain the mean bundle tenacity. The results of efficiency at first unit rupture are plotted as the solid lines of Figure (10). Here N is the number of units in the bundle and $M = b\sigma$ where σ is the standard deviation of the unit elongation to break and b is the slope of the assumed linear average stress-strain curve of the units in the region near rupture.

In attempting to extend this reasoning to larger size bundles, another problem is encountered, namely, that maximum load does not necessarily occur when the first unit breaks. In fact, for large numbers of units a very sizeable portion may be broken before maximum bundle load is attained. This case has been discussed in previous work (1,2), and the results of this previous work bracket the middle-sized groups. Thus the problem is reduced to the specific solution of some examples of middle sized groups in order to extend the analysis of the effects of variability over the entire range from single units to infinitely large bundles. The important practical results of these calculations will be both the ability to predict the effects of number of units and also to define the minimum size which constitutes an "infinite" size for tensile strength purposes.

An elongation is chosen for the first unit to break, and the probability of having the maximum bundle strength occur at this point is calculated. A number of other elongations for first unit rupture are chosen and similar probabilities calculated. The results are plotted as a distribution of probability of occurrence of maximum load versus elongation at first unit break.

Then similar sets of calculations are made for the cases where maximum bundle strength is attained when the second unit ruptures, third unit ruptures, etc. The method is outlined in detail in Appendix (I) and the results for $N = 4$, i.e.; a bundle of 4 units, and $M = 20$ are plotted in Figure (9). The parameter M is a convenient one to describe bundles(6). It is numerically equal to $b\sigma$ or be_mV where b is the slope of the linear approximation to the average unit stress-strain curve near rupture; σ, the standard deviation of elongation to rupture; e_m, the mean rupture elongation; and V, the coefficient of variation of elongation to rupture of the units.

The relative areas under the curves of Figure (9) represent the relative frequencies of maximum bundle loads occurring at the first, second, and third unit breaks. Clearly, any break beyond the third has a very small probability of producing a maximum bundle load and need not be considered. The average breaking elongation can be calculated by taking the weighted mean of all of the distribution curves, that is, the sum of each of the individual means times the area under the curve, divided by the sum of the areas. To find the average breaking load, the mean breaking load for each configuration must be modified by the number of units intact. Strictly speaking, the total area should be numerically equal to unity, but since in calculating averages the same normalization constant appears in both numerator and denominator, formal normalization is unnecessary here.

FIGURE 9

RELATIVE FREQUENCY OF MAXIMUM BUNDLE LOAD vs t

n = 4, m = 20

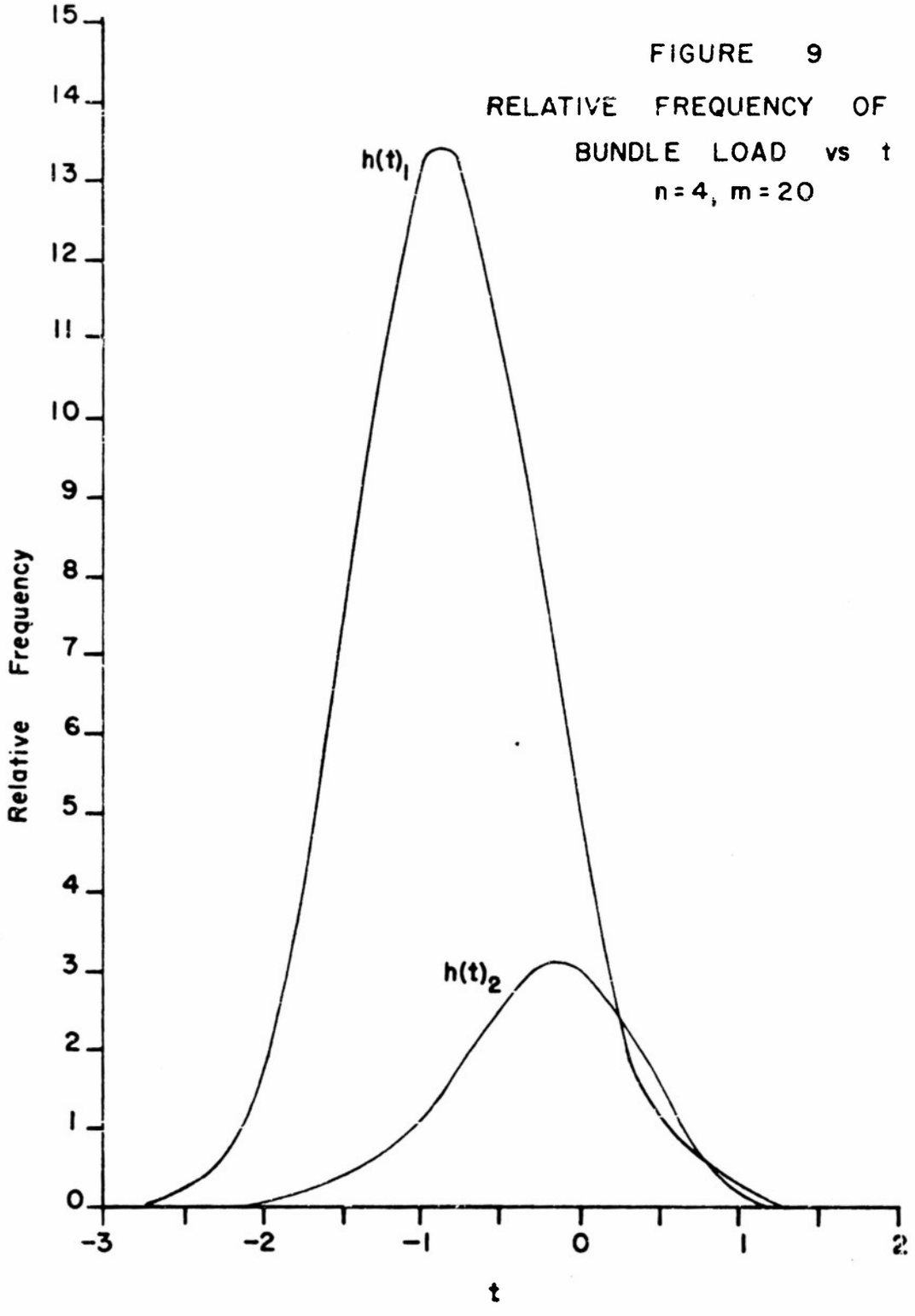

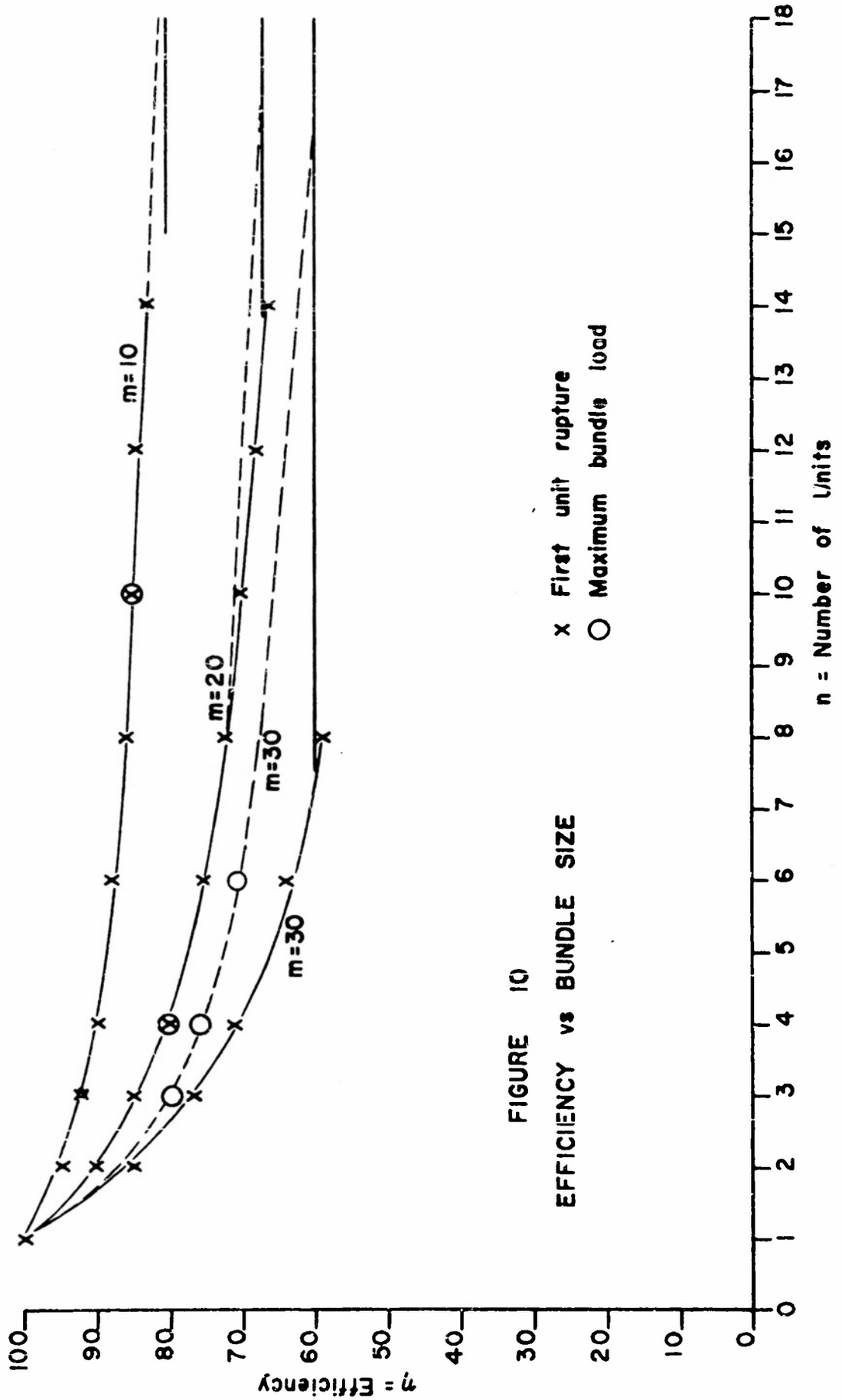

FIGURE 10

EFFICIENCY vs BUNDLE SIZE

The same procedure was followed for other values of N and M. Combining this information with both the translational curves for first unit breaks, and also the magnitude of bundle efficiencies for very large groups of units, a useful graphical representation can be made as follows: It is known that the effect of variability on the mean increases with increasing size of group and thus must asymptotically approach the value found for very large sized groups. It is also known that the effect can be no greater than that corresponding to the first unit break, since the elongation at maximum load can be no less than that where the first unit breaks. Thus, a translational efficiency curve for bundles, plotted versus N, the number of elements in the bundle, must lie or or above the curve giving the efficiencies under the assumption that maximum strength is reached when the first unit breaks. Then the general shape and position of the translational efficiency curves are known and by calculation of only a few judiciously selected points as above a general set of curves showing translational efficiency of the bundle versus N, the number of units in the bundle can be plotted. This has been done in Figure (10), where the curves are represented by the dashed lines. The solid lines of Figure (10) represent the results for first unit break.

There are three important points to note in these curves: 1.) As N becomes smaller, the efficiency can be more nearly characterized directly by the curve of efficiency at first unit break. 2.) As N reaches about 15, the assymptotic value can be used with very little error or, in other words, a very large sample can be assumed. 3.) With other factors remaining constant, the efficiency of translation is inversely functional with the number of units in the bundle for small numbers of units. These observations must be interpreted with caution because they apply only to translation of strength, although they are based on elongation. That is, it is proper to say that strength-wise a bundle of 15 units from a given population will on the average translate to about the same extent as a bundle of 100, but it is not true that the average breaking elongation will be the same for the two cases. This can best be understood by following the steps of the derivation given in Appendix (I).

The analysis of a plied yarn containing a core differs from the analysis of similar number of units in parallel since in the former case any significant ply helix angle imposes a different strain on the core yarn than on the exterior yarns. The statistical analysis must take this difference in strains into account. This has been done for seven ply yarns, with the procedure outlined in Appendix (III), and the results of the analysis given by the efficiency curves of Figure (11). An interesting feature of these curves is the relative insensitivity of the results to unit variability for any significant ply helix angle. This is true only for the range of unit variabilities covered by the calculations. The cause of this apparent insensitivity resides in the somewhat improved degree of elongation balance between the core yarns and the exterior yarns with a small increase in unit variability. Such an effect would be difficult to demonstrate experimentally since the magnitude of the effect is small. In the case of a large number of exterior yarns with a single unit core, as indicated later, little error is introduced by assuming all units to be in parallel.

FIGURE 11

THEORETICAL TRANSLATIONAL EFFICIENCY OF SINGLES INTO 7-PLY YARN vs SINGLES RUPTURE ELONGATION VARIABILITY

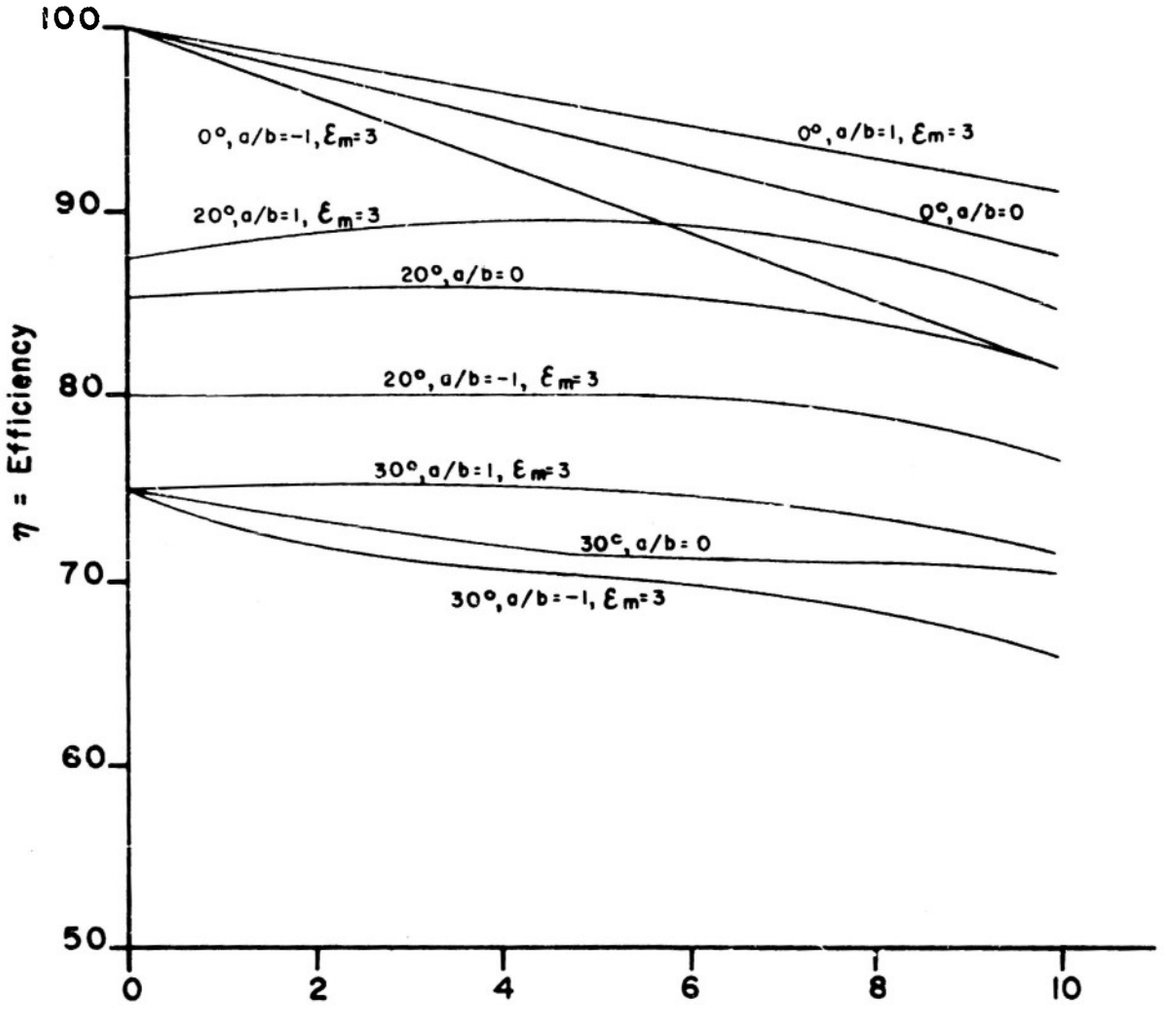

It is of interest to note that the curves of strength translation at first unit break can also be interpreted as giving the average strength of the weakest link in chains composed of n links. Here the work link means simply some arbitrary length of fiber, yarn, or plied yarn. In parallel type structures all elements are at a known elongation, so elongation has been chosen as a basic parameter. In series structures, all elements are at the same load, so load must replace elongation in the statistical calculations. The solid curves of Figure (10) with m replaced by the coefficient of variation of breaking load will give directly the efficiency of units in series where the abscissa is the number of units in series. For example, it should be possible to determine the effect of gage length on tensile strength simply by knowing the mean strength and standard deviation of strength at some short length and assigning to this length an n of 1. The strength at any longer gage length could then be calculated from the efficiency curves given in Figure (10) if the only effects of gage length were statistical in nature. However, differences between specimens in the short gage length tests might be due to factors which would not have acted on a single long specimen and thus obscure the results, e.g., rate of loading, jaw penetration effects, etc.

III. COMPARISON OF THEORY WITH EXPERIMENT

A. Excess Lengths in Yarns Removed from Strand

It has been shown theoretically that the length of a fiber in a circular yarn should vary according to the inverse cosine of the angle it makes with the yarn axis, or in terms of helical parameters:

$$l_f = l_y \sqrt{1 + 4\pi^2 N_y^2 r^2}$$

where l_f is the length of fiber corresponding to a length l_y of yarn, N_y is the number of turns per unit length of the yarn, and r is the fiber distance from the yarn center.

Tests have been performed in which a 20 inch length of yarn is placed under a constant tension, completely untwisted, and all non-throughgoing fibers removed. Then one by one the taut fibers are cut and the increased length of the yarn measured several times during the cutting procedure. The per cent of the total fibers cut is plotted versus the per cent increase in length. The theoretical form of such a curve can be derived as follows:

Consider a circular yarn of radius R_y. Then the per cent of fibers included to a radius r is $\frac{\pi r^2}{\pi R_y^2} \times 100 = 100 \frac{r^2}{R_y^2}$, assuming a constant yarn density from the center outward. The length of a fiber at a radius r = $l_y \sqrt{1+4\pi^2 N_y^2 r^2}$ and the per cent increase in length is:

$$\frac{l_y \sqrt{1 + 4\pi^2 N_y^2 r^2} - l_y}{l_y} \times 100 = \left(\sqrt{1 + 4\pi^2 N_y^2 r^2} - 1\right) 100 \quad \text{---------- (22)}$$

For small values of $4\pi^2 N_y^2 r^2$, $\sqrt{1+4\pi^2 N_y^2 r^2}$ can be closely approximated by $1+2\pi^2 N_y^2 r^2$, so that the expression for per cent increase in length becomes $100(1+2\pi^2 N_y^2 r^2 - 1) = 200\pi^2 N_y^2 r^2$. The plot then becomes a straight line with slope $100 \frac{r^2}{R_y^2}$. This can be expressed in terms of the yarn surface helix angle θ_y as $2 \operatorname{ctn}^2 \theta_y$.

$$\frac{\frac{r^2}{R_y^2}}{200\pi^2 N_y^2 r^2} = \frac{1}{2\pi^2 N_y^2 R_y^2}.$$

If a yarn is partially untwisted by, say, plying, after having been

spun to an initial twist which gives a helix angle θ_{yo}, it is clear that the distribution of absolute fiber lengths should still be the same as before untwisting. However, the theoretical length distribution for a yarn with the new lower angle θ_y, will have a steeper slope. The difference in slopes for the original and untwisted yarn is a measure of the excess fiber lengths existing in the untwisted yarn. The distribution of these excess lengths with respect to radius has been derived in Section I, C.

Figure (12) shows a plot of four theoretical distributions of fiber length together with the experiments results for a "soft" twist yarn series. A detailed description of the nature of these samples will be given later. However, for convenience in following Figure (12), the symbol YS refers to a yarn (Y) before plying whose twist was"soft" (S). All three letter symbols refer to yarns from strands, the first letter Y representing the fact that the test was performed on yarns from strands where the original yarn twist was soft (the second letter S), while the strand twist was in turn soft (third letter S), medium (third letter M), or hard (third letter H). Thus, as the designation of yarns from strands proceeds from YSS to YSH, the required fiber length should decrease, and thus the excess length should increase. In each case experimental lengths of fibers in yarn removed from strands, as well as theoretical lengths, were determined using the singles twist as it lies in the strand. While experimental results of fiber length are not dependent upon the manner in which the singles yarns were untwisted from the strands, the twists to be used in calculating the theoretical lengths are so dependent.

The results of Figure (12) can be seen to agree with theory quite well so far as the trend is concerned. The four experimental curves are all nearly identical, irrespective of final twist, as would be expected for yarns of originally the same twist. The theoretical distributions indicate the distribution which would be required in order that all the helical paths be exactly satisfied with no excess lengths, and thus that the excess lengths increase with increasing twist removal, achieved by increasing the strand twist. The discrepancy between theoretical and experimental curves for the original YS yarn are probably due to errors in both experiment and assumption: 1.) experimental - it is possible that not enough tension was exerted on the yarn when a large percentage of the fibers were still intact, so that the increase in length measured was too low. For example, at the 60% ordinate of Figure (12), the length increase is about 0.4% too low. On a 20" gage length this means 0.08", a small amount for a rough measuring and tensioning system; 2.) theoretical - the assumption that all fibers lie in perfect helices is clearly not true since much darting has been observed. While this darting is of little consequence over the short lengths involved in yarn rupture, it will have a tendency to equalize fiber lengths over the longer lengths used in the investigation of fiber length distributions and thus yield a steeper slope than that calculated. The long tails observed in the upper regions of the experimental curves are undoubtedly due to the tendency of a very few fibers in every yarn to be somewhat stray, that is, not really tightly bound within the yarn.

If the above reasoning is true, then the major deviation between theoretical and experimental results has been explained on the basis of length,

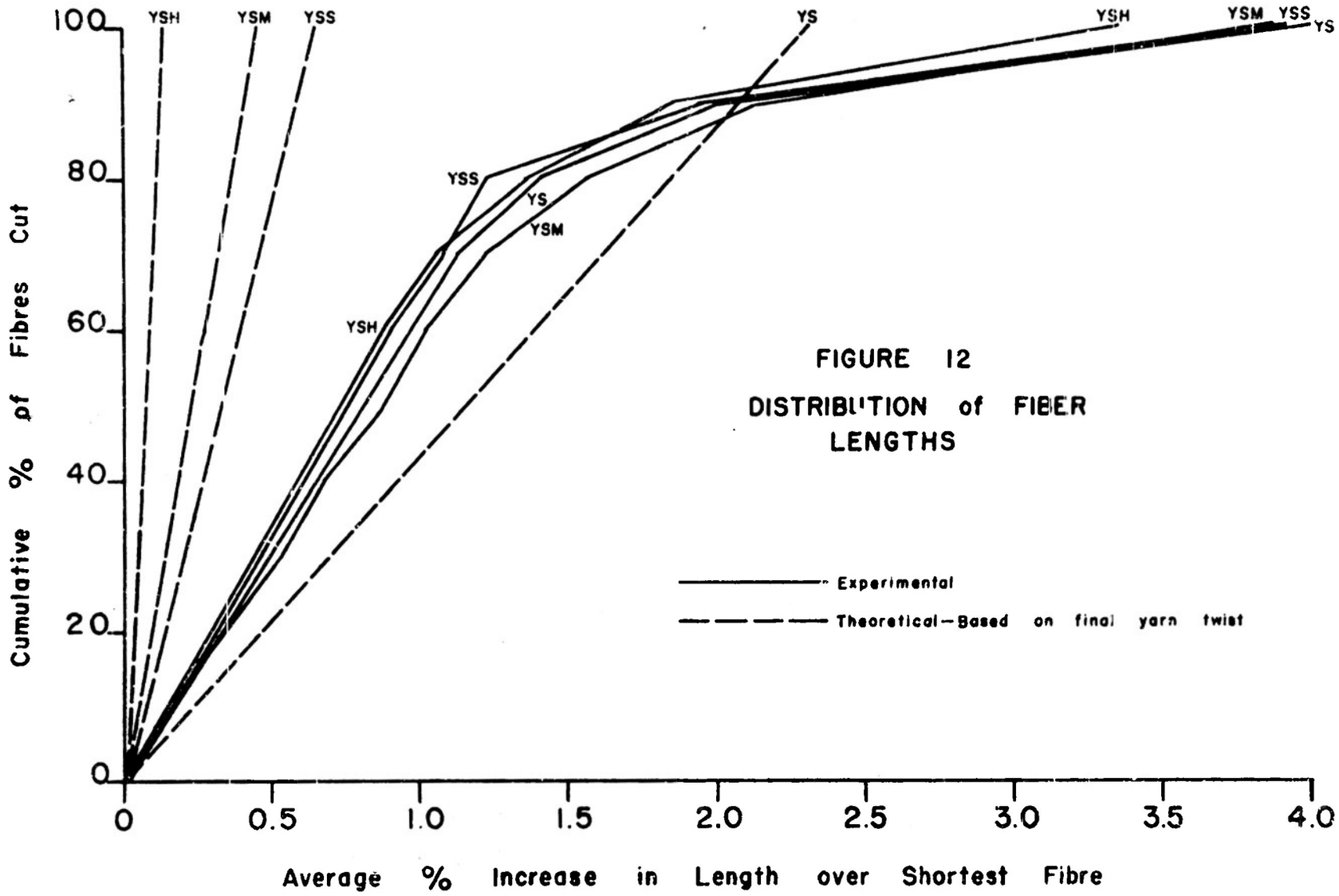

FIGURE 12

DISTRIBUTION of FIBER LENGTHS

a consideration not valid for the short lengths involved in rupture, and thus tensile calculations should be based on the more accurate theoretical values and not the experimentally obtained curves.

B. Strength of Yarns Removed From Strands

In Section II-C, a theoretical analysis was made of the strength of yarns removed from strands on the basis of the creation of excess lengths due to untwisting in the stranding operation.

As part of the study of factors influencing the translational efficiency of cordage, a series of Abaca fiber cordage strands of different twists made from yarns of different twists were produced at the Boston Navy Yard. The description of pertinent nominal structure of these strands is given in Table I. In all cases strands possess a single core yarn surrounded by either 13 or 14 singles yarns in the exterior shell. For purposes of efficiency calculations of yarns removed from strands, there is negligible effect produced by changing the numbers of external yarns. Correspondingly, there is negligible difference in residual singles twist whether a core yarn or external yarn is used, i.e., it is impossible to experimentally detect such differences.

TABLE I

TWIST STRUCTURE OF EXPERIMENTAL ABACA STRANDS
All yarns 300 ft./lb. nominal weight

Strand Code	Singles Yarn Twist Before Stranding (turns/ft.)	Strand Twist (turns/ft.)	Singles Yarn Twist As It Lies In The Strand (turns/ft.)
SSS	6.6Z	4.38	3.5Z
SSM	6.6	5.4	2.9
SSH	6.6	6.9	1.7
SMS	11.0	3.8	9.0
SMM	11.0	4.8	8.4
SMH	11.0	6.0	8.0
SHS	15.0	3.9	13.4
SHM	15.0	3.9	13.4
SHH	15.0	4.3	13.3

In all cases, the singles twist as it lies in the strand was determined by cutting away all but one of the yarns in the strand, followed by untwisting of the single remaining yarn. Length growths were added to original strand lengths so that the twist per unit length of yarn could be determined. The foregoing procedure is obviously equivalent to removing a

single yarn from the strand by "unwrapping", i.e., holding one end of the strand rigidly clamped, and rotating the free end of any yarn about the strand axis but not it's own axis. By this latter technique, most of the yarns in any given length of strand can be used for twist determinations. As will be shown later, the twist of yarn determined by either of the two described procedures gives helix angles and excess lengths of yarns as they lie in strands substantially in agreement with those which result from the more rigorous analyses of Schwartz (4) and Chow (5). Yarns removed from the strands described in Table I are designated as YSS, YSM, etc., the initial letter Y, for yarn, replacing the initial letter S, for strand.

The results of efficiency calculations for the full series of soft, medium, and hard twist yarns removed from soft, medium and hard twist strands together with the theoretical efficiencies, with and without consideration of excess lengths are tabulated in Table II. These results were calculated by the summation procedures derived in Section II-C. The plus and minus values represent two standard errors of efficiency calculated using only the variance in experimental strand strengths.

TABLE II

COMPARISON OF THEORETICAL AND EXPERIMENTAL EFFICIENCIES OF YARNS FROM STRANDS

Yarn* Code	Initial Yarn Twist (turns/ft)	Final Yarn Twist (turns/ft)	Yarn Diameter (inches)	Efficiencies, Per cent		
				Theoretical No excess Lengths	Theoretical Full excess Lengths	Experimental
YSS	6.6Z	3.5Z	0.125	58.8	54.0	53.6±6
YSM	6.6	2.9	0.125	58.8	53.2	44.0±5**
YSH	6.6	1.7	0.125	58.8	51.2	36.3±5**
YMS	11.0	9.0	0.125	56.3	49.5	46.2±4
YMM	11.0	8.4	0.125	56.3	47.0	46.2±1
YMH	11.0	8.0	0.125	56.3	45.2	44.0±3
YHS	15.0	13.4	0.100	54.7	47.8	42.9±5
YHM	15.0	13.4	0.100	54.7	47.8	33.5±3
YHH	15.0	13.3	0.100	54.7	47.8	42.9±4

* First letter indicates yarn, second letter twist of yarn, third letter twist of strand.
** See text for explanation of these values.

The experimental values of efficiency for the YSS, YMS, YMM, and YMH yarns are all quite close to the theoretical values computed for full excess-lengths. In the case of yarns YSM and YSH the theoretical values are too high

since the residual yarn twists are sufficiently low that only the throughgoing fibers contribute any appreciable amount to the strength, although the non-throughgoing fibers contribute more load in yarn YSM than in yarn YSH, since the residual twist in the former exceeds that in the latter. While no precise quantitative prediction of the strengths of these yarns can be made, it is possible to account for most of the discrepancies as follows: for the gage length to fiber length ratio employed in the determination of experimental efficiencies approximately one-third of the fibers were not throughgoing. Thus, considering only those fibers which are throughgoing, the efficiency of yarn YSH would be $\frac{2}{3} \times 51.2 = 34.1\%$. Some strength would be anticipated for the non-throughgoing fibers in this yarn, but the magnitude would be small and contributing to the efficiency in the order of $36.3-34.1 = 2.2\%$. For the YSM yarn, where the residual twist is higher, the contribution of the non-throughgoing fiber to efficiency is probably of the order of $44.0-\frac{2}{3} \times 53.2 = 8.5\%$, higher than the YSH yarn as would be anticipated. However, as these yarns lie in the strand, additional cohesive forces are created by the strand twist, and thus the low experimental singles strength for yarns YSM and YSH should not be construed as indicating that the strands which they comprise would be weak.

For the hard twist yarn series, YHS, YHM, and YHH the discrepancies are higher than could be accounted for on the basis of experimental strength variation, just slightly in the case of YHS and YHH and considerably in the case of YHM. A possible explanation for the discrepancies in the cases of yarns YHS and YHH is that the experimental values of initial twist, N_{yo}, and final twist, N_y, for these yarns were not sufficiently accurate. From previous work it might be concluded that a small variation in twist for moderate helix angle yarns would not effect the strength very much, and this is the case where twist effects are mostly angular in nature. However, when excess lengths are considered, the effect of a small change in twist may by no means be small. As an example, the theoretical strength of a yarn removed from strand with excess lengths present has been calculated on the assumption of initial yarn twist of 13.4, 15, and 17 turns per foot, and a final yarn twist of 13.4 turns per foot. The 15-13.4 combination corresponds to the actual as measured and calculated hard twist series. The results are plotted in Figure (13). Over the range covered, it can be seen that the rate of change of efficiency with initial twist is about 5% per turn per foot of twist. The rate with respect to final twist is about the same for this range. Thus the effects of small twist variations are of the order of the discrepancy.

No similar reasoning can explain all of the very large difference between theoretical and experimental values of efficiency for the YHM yarn, nor for the large difference between this yarn and the other two yarns of the hard yarn twist series. On the basis of all parameters considered theoretically, as well as their measured structural geometries, the three yarns are very nearly identical. All that can be said for yarn YHM is that some factor such as fiber tenacity, which was not measured for each construction, does not have the value ascribed to it on the basis of previous investigations.

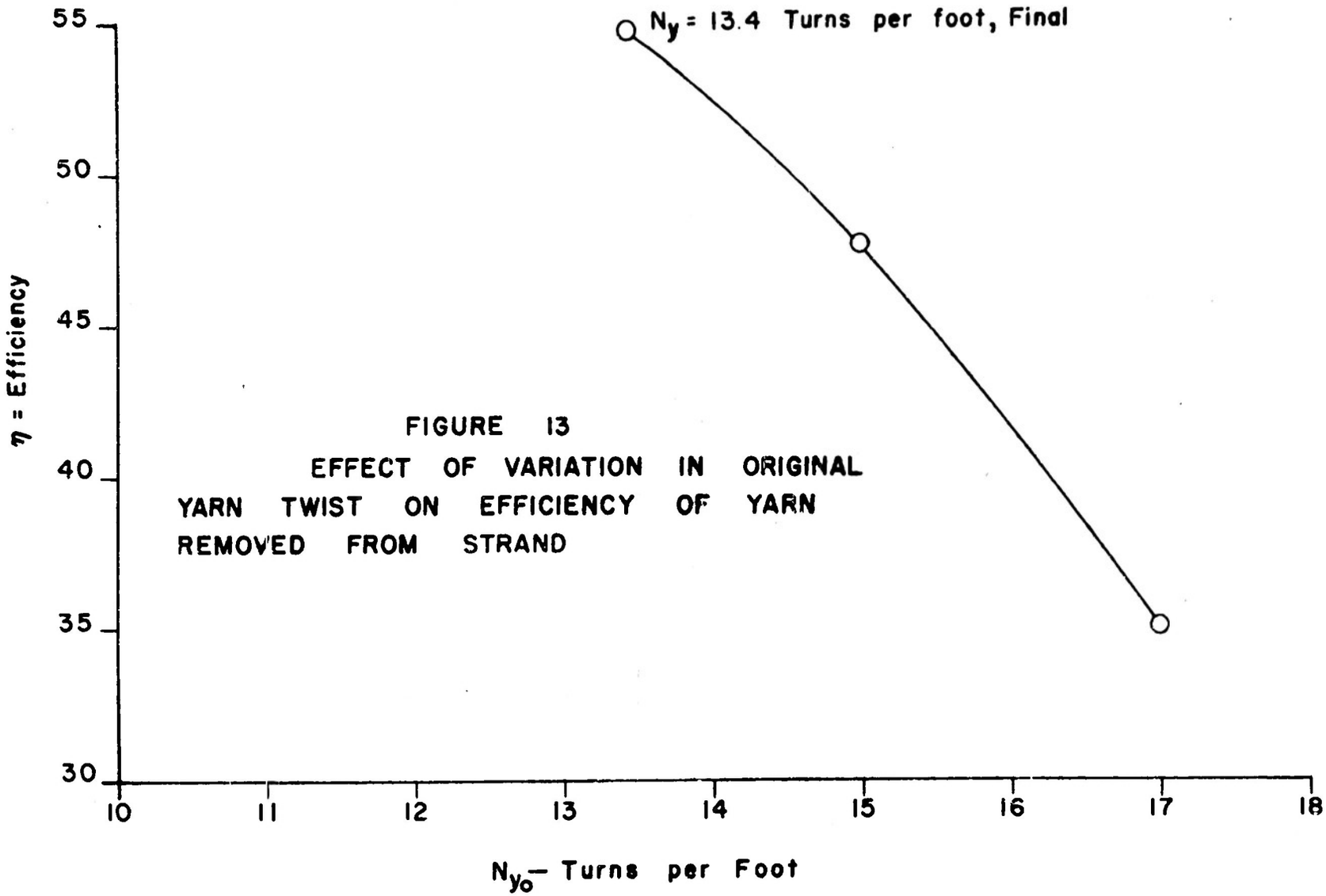

FIGURE 13

EFFECT OF VARIATION IN ORIGINAL YARN TWIST ON EFFICIENCY OF YARN REMOVED FROM STRAND

In a subsequent section on strand efficiency it will be shown that the foregoing discussion on excess lengths may be largely of academic interest since the condition of circular symmetry of the yarn is strongly violated as the yarns lie in strands. Thus yarns removed from strands do not possess the same characteristics as they do when they lie in the strand, although it is very probable that some residue of large excess lengths are present in yarns as they lie in strands.

The physical reason for excess lengths which are created by partial untwisting of a yarn influencing efficiencies so profoundly is that they accentuate the degree of unbalance of elongations amongst fibers in a yarn. The exterior fibers, which by virtue of the helix angles are under a lesser strain than the interior fibers, can be subjected to non-load-bearing extension as a result of the excess lengths. Obviously, this non-load-bearing extensibility would exert less effect for a high elongation fiber or for a fiber whose stress-strain curve was flat over a wide range of elongations near rupture, i.e., a high a/b. The converse of this effect of excess lengths is also of interest. For example, it is possible from the theoretical data given in Technical Report Number 6 to determine the maximum possible efficiency of a yarn if all of the elongation unbalance between fibers were removed. Such a hypothetical structure might be visualized, by, say, imagining varying amounts of crimp to be inserted amongst the fibers. The amount of crimp should diminish from inside to outside of the yarn. For such a yarn, the efficiency would be determined from:

$$\eta_y = \eta_{bundle} \frac{\ln(\sec^2 \theta_s)}{\tan^2 \theta_s} \qquad (23)$$

whereas η_{bundle} is the bundle efficiency for the type of fibers under consider- and θ_s is the surface helix angle of the yarn. In general, efficiencies calculated from Equation (23) are higher than those given in Technical Report Number 6, indicating that increases in strength could be achieved by adjusting crimps. However, the extent of such improvements are sizeable only for stiff inextensible fibers whose rupture elongation variability is low. A coefficient of variation of fiber elongation to rupture of 10% is sufficiently large to mask the strength increase. It is also clear that the extra yarn weight per unit length resulting from the insertion of crimps as described above would act to diminish the efficiency.

C. Relationship of Initial to Final Twist in Yarns Removed From Strand

In Section I-B it was shown that in the normal stranding procedure the relationship between final singles twist N_{yp}, initial singles twist N_{yo}, strand twist N_s, and helix angle θ_p should be:

$$N_{yp} = N_{yo} - N_s \cos \theta_p \qquad (24)$$

Table III gives N_{yp} as determined from the above equation and also as measured directly for the series of yarn whose efficiencies were compared in Table II.

TABLE III

COMPARISON OF CALCULATED AND EXPERIMENTAL YARN TWISTS FOLLOWING STRANDING

Yarn Code	N_{yo} (TPF)*	N_s(TPF)	Cos θ_p	l_s/l_y	Final Yarn Twist, N_{yp}(TPF) Calculated	Experimental
YSS	6.6Z	4.38	0.931	0.930	2.6Z	3.5Z
YSM	6.6	5.4	0.897	0.887	1.7	2.9
YSH	6.6	6.9	0.880	0.858	0.5	1.7
YMS	11.0	3.8	0.945	0.944	8.4	9.0
YMM	11.0	4.8	0.917	0.918	6.6	8.4
YMH	11.0	6.0	0.878	0.857	5.7	8.0
YHS	15.0	3.9	0.943	0.934	11.3	13.4
YHM	15.0	3.9	0.942	0.929	11.3	13.4
YHH	15.0	4.3	0.931	0.926	11.0	13.3

*TPF = turns per foot of twist.

The column headed cos θ_p given the cosine as calculated by the method described in Section I-A. The l_s/l_y column gives the ratio of the length of the strand to the length of the yarn contained in that length. Theoretically l_s/l_y = cos θ_p and agreement between there two quantities is very good, the discrepancy always being less than 3%. Unfortunately, the agreement between calculated and theoretical values for N_{yp} is very poor, indicating that Equation (24) is not a valid representation of what happens to twist during the stranding operation. There is no obvious reason why singles turns are not removed on a one-to-one basis with strand twist, but clearly they are not. For lack of concrete evidence to support any quantitative explanation, this problem will be left for future exploration making it necessary to determine final yarn twists experimentally. It should be pointed out here that the use of the more rigorous analysis of plied yarn structure as developed by Chow (5) does not produce sufficiently different results from Equation (24) to account for the differences in Table III.

D. Strand and Plied Yarn Efficiencies

Theoretical formulation of the factors involved in the translation of yarns into higher order structures is somewhat complicated by the inability to accurately characterize the properties of yarns as they lie in such higher order structures. Fortunately, certain approximating assumptions can be made which simplify calculation and yet yield results which check experimental values to within the range of experimental error.

By utilization of the concepts developed earlier in this report, strand or plied yarn efficiency can be calculated from the integration of the following data and assumptions:

1.) Average stress-strain curve of yarns as they exist in the strand or plied yarn.

2.) Variability of elongation to break of yarns as they lie in the higher order structure.

3.) Strand twist and yarn position.

4.) The assumption that any yarn supports negligible load after attaining maximum load, i.e., that the yarn ruptures completely.

It has been shown that for parallel units the curves of Figure (10) may be expected to give the multiplication factor required to account for the effects of variability among yarns. To test the accuracy of this assertion, consider the case of bundles containing different numbers of fibers as a special case of a higher order structure. For this special case the stress-strain curve of the fibers as they lie in the bundle is, clearly, the same as if they were single. Similarly the variability of fiber elongation to break is unchanged by the bundle formation. There is no twist, and rupture of the individual fibers is sudden and complete. Thus only 1 and 2 above apply and the pertinent data for both are unambiguously defined. Listed below in Table IV are the experimental and theoretical results for efficiency of translation of bundles each of which contain "small" numbers of Manila abaca fibers. Theoretical efficiencies are based on the efficiency curves of Figure (10).

TABLE IV

EFFICIENCIES OF TRANSLATION OF MANILA ABACA FIBER STRENGTH INTO BUNDLES CONTAINING A SMALL NUMBER OF UNITS

Number of Fibers in Bundle	Efficiencies, %	
	Theoretical	Experimental
2	90	88.3±7
3	81	81.0±5
7	73	76.0±8
15	68	69.8±7.5

The theoretical values given above were calculated from pertinent fiber data of: $b = 42.5$, $e_m = 2.47\%$, and $V = 24\%$; or $m = 25.2$; as determined from 75 single fiber tests. The units of b are percent of mean ultimate fiber strength per percent elongation. Experimental results are listed in Table IV with a range of ± two standard errors calculated considering only the variance in bundle strength. On the basis of the excellent agreement given in Table IV there is no reason for not accepting the curves of Figure (10).

A twisted structure with all units lying at the same angle with respect to the structure axis presents no theoretical complexity. Final efficiency for this case would be determined by multiplication of bundle efficiency by the cosine of the angle of inclination for the component of force and again by a cosine of the angle for denier increase due to the twist takeup. The problem, as stated above, is that no yarn parameters are available for the yarn as it lies in the strand or plied yarn. These parameters must be estimated from consideration of single yarn properties outside the strand and the assumed effects of lying in a strand.

Probably the two most important effects of stranding on the singles other than the change of turns of twist, which change can be measured, are:

1.) Increase of cohesive force between fibers, and;

2.) Distortion of the circular cross-section.

The increase in cohesive force is of importance principally in low twist singles whose twist, if the yarn were removed from the strand, would be below optimum. Distortion of the circular cross-section of the yarn can have a very great effect on cancelling some of the adverse effects of both excess fiber lengths and stress concentrations which would exist in a strand whose yarns were circular. This latter point, i.e., stress concentration, is discussed later in this report. It was stated earlier herein that a careful analysis of the strength of a yarn with excess lengths was largely of academic interest since such a configuration does not exist within a stranded structure. Thus, while the analysis of yarns removed from strands, calculated considering the existence of excess fiber lengths is probably valid, it is of little use

in the calculation of strand strengths and efficiencies.

Before presenting the results of calculations on strand and plied yarn strengths, an analysis of some of the effects of cross-section distortion on removal of excess lengths will be made. This analysis will help to clarify the reasonableness of certain of the assumptions which are made and thus justify them.

Consider the case of a yarn of circular cross-section containing no excess fiber lengths. The yarn will exhibit a moderately firm hand. Now visualize a partial untwisting of the yarn. From the preceeding analysis of Section I-C it is known that excess fiber lengths will exist within the yarn and clearly the yarn will feel less firm

If several of these yarns were twisted together there would obviously be a tendency for the circular yarn cross-section to distort, and it is well known that such sections are in general not circular in plied and stranded structures. The question now arises as to what effect this distortion will have on the tensile properties of the yarn as it lies in the strand. Two possible effects on yarn structure are:

1.) Changes in the required path length of the fibers and, thus, in the excess fiber lengths.

2.) Changes in inclination of the fibers.

To see how little yarn cross-sectional shape distortion may change fiber helix angles while having a significant effect on excess fiber lengths, consider the case of a yarn of circular section and helix angle of θ_c. Now distort the section to a square. Under the assumption of equal packing factors, the analysis is as follows:

Let:

A = the cross-sectional area of the yarn, same for both round or square yarn.

N = turns of twist per unit length.

r = radius of yarn.

S = length of side of square.

Then:

$$A = \pi r^2 = S^2$$

$$S = r\sqrt{\pi}$$

Since the fiber progresses an axial distance of $\frac{1}{N}$ for every complete turn, on one side of the square cylinder it will progress $\frac{1}{4N}$. (See Figure 14)

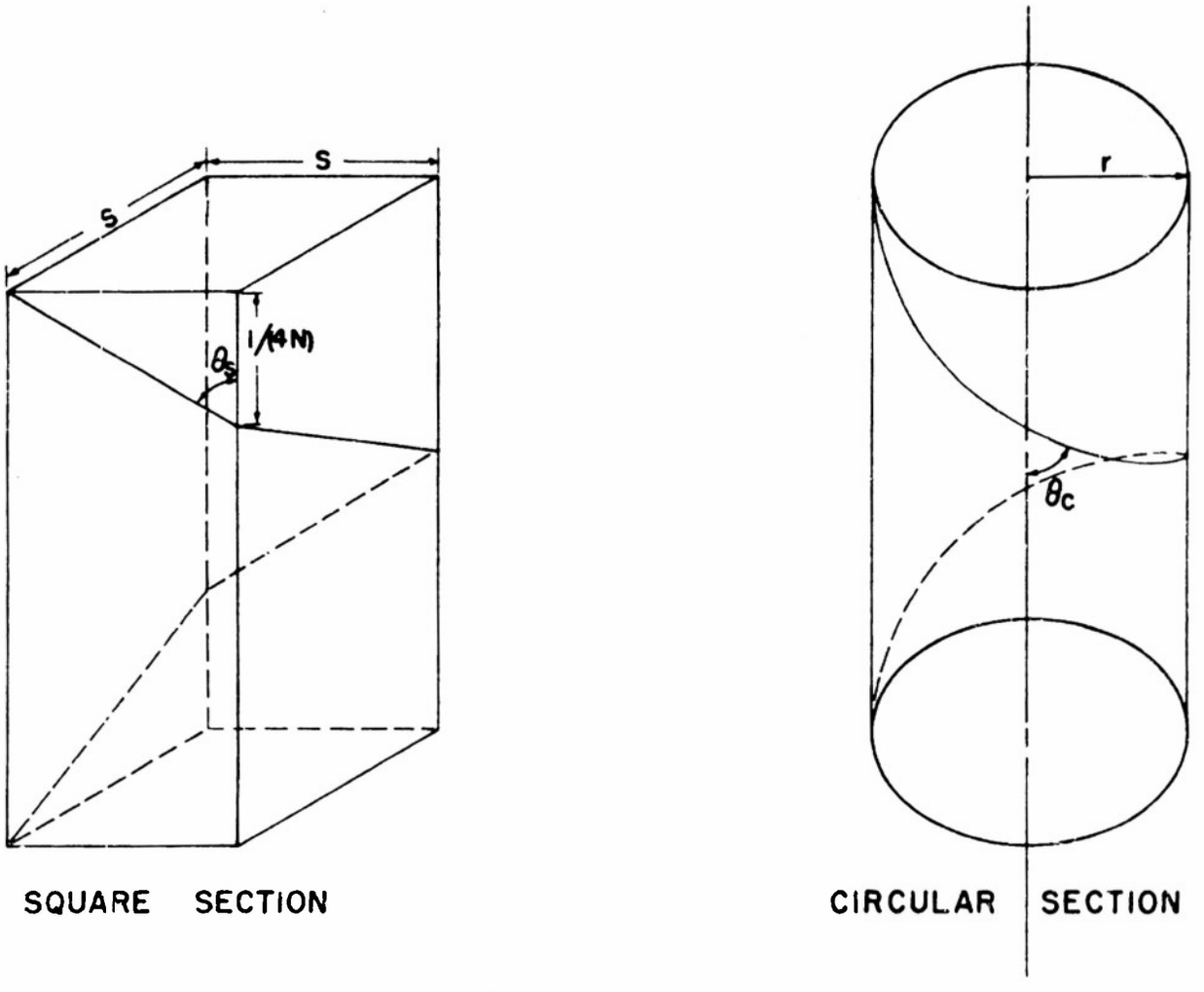

FIGURE 14

ILLUSTRATION OF SQUARE AND CIRCULAR HELIXES

The length of fiber in one turn about the circular helix is:

$$l_c = \frac{1}{N}\sqrt{1 + 4\pi^2 N^2 r^2}$$

$$= \frac{1}{N}\sqrt{1 + \tan^2\theta_c}$$

while about the square cylinder it is:

$$l_S = 4\sqrt{S^2 + \left(\frac{1}{4N}\right)^2}$$

and since $S = r\sqrt{\pi}$, this becomes:

$$l_S = \frac{1}{N}\sqrt{1 + 16\pi N^2 r^2}$$

$$= \frac{1}{N}\sqrt{1 + \frac{4}{\pi}\tan^2\theta_c}$$

The percentage change in required path length is:

$$100\ \frac{l_S - l_c}{l_c} = 100\left[\frac{\frac{1}{N}\sqrt{1 + \frac{4}{\pi}\tan^2\theta_c} - \frac{1}{N}\sqrt{1 + \tan^2\theta_c}}{\frac{1}{N}\sqrt{1 + \tan^2\theta_c}}\right]$$

$$= 100\left[\frac{\sqrt{1 + 1.277\tan^2\theta_c}}{\sqrt{1 + \tan^2\theta_c}} - 1\right]$$

The fiber helix angle on the surface of the square cylinder is given by:

$$\tan\theta_S = \frac{S}{1/4N} = 4Nr\sqrt{\pi} = 7.092\,Nr$$

Since the fiber helix angle on the surface of the circular cylinder is given by:

$$\tan\theta_c = 2\pi Nr = 6.283\,Nr$$

then:

$$\tan\theta_S = 1.129\tan\theta_c$$

Figure (15) shows the relationship between original helix angle, final angle, and decrease in length according to the condition and analysis above.

FIGURE 15
EFFECT OF DISTORTION TO SQUARE SECTION ON EXCESS LENGTHS AND HELIX ANGLE

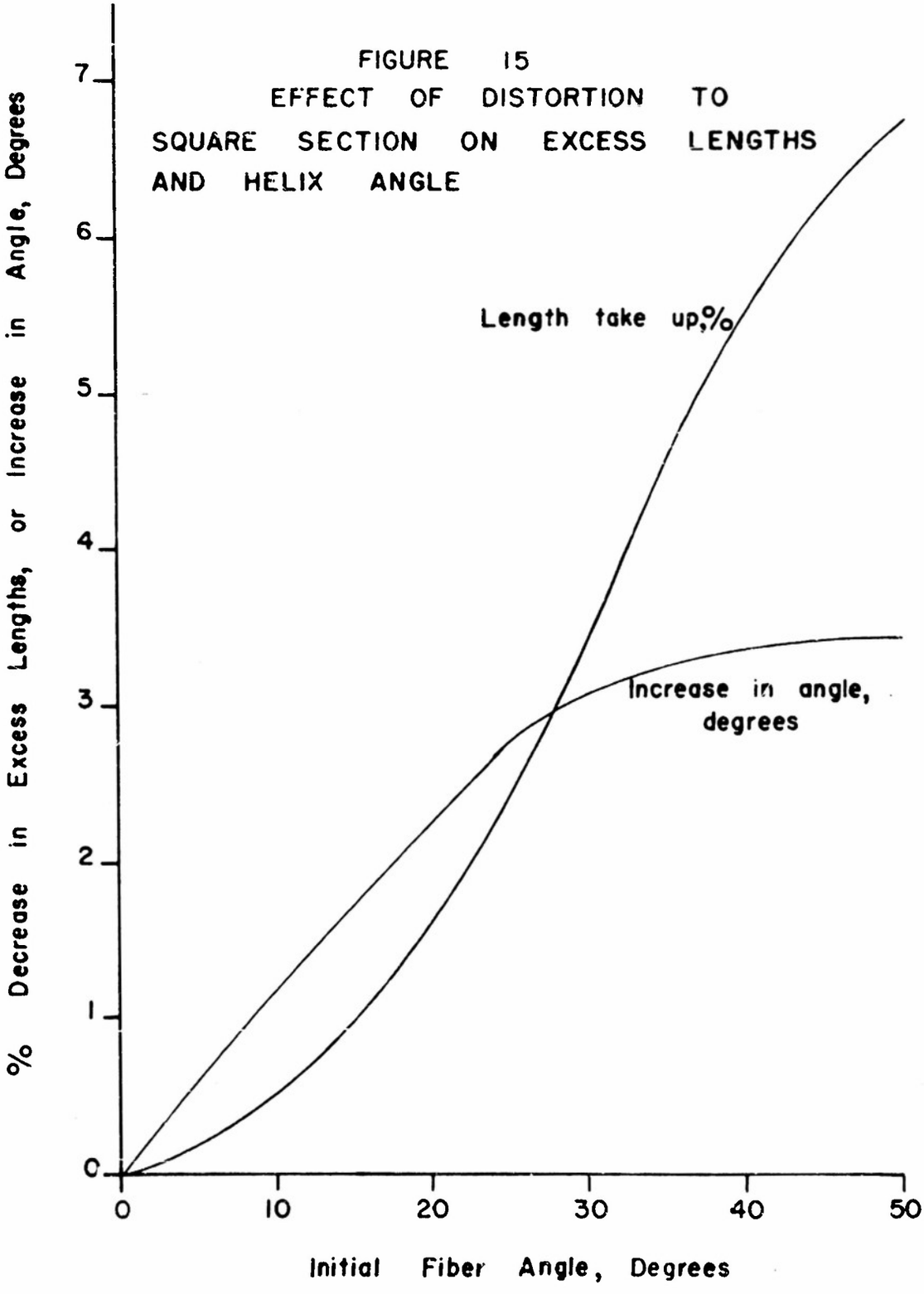

Even for a helix angle of 30°, which is higher than would normally exist in a yarn, the change in angle is only about 3°. Reference to the curves of translational efficiency given in Technical Report Number 6 will show that this in itself will not occasion any very great change in efficiency. However, corresponding to this angular change there is a length takeup of about 3.4%, an amount which is sizeable in most considerations of excess lengths. For angles as low as 15°, the length takeup is nearly 1%. This may be quite significant in low elongation to break materials.

The square section is, of course, hypothetical. The actual shape of the final section will be determined by a number of things, chiefly the number of yarns, the strand twist, the yarn twist, and yarn excess lengths. Clearly the resistance to distortion would be quite large after the excess lengths had been removed from any appreciable number of fibers. Thus a yarn with low excess lengths would be expected to maintain itself more nearly circular.

While an analysis of the many possible distorted shapes is not practical, it can be said without reservation that any appreciable distortion from a circular shape will, unless accompanied by a large increase in packing factor, cause a takeup of excess fiber length. This distortion will continue to the point where enough excess lengths are fully removed to make further distortion impossible with the forces available from the plying or stranding operation. The distortion is accomplished with little change in angle of inclination. While this information is not very definitive, it does make it reasonable to assume that yarns with small amounts of excess length will show virtually no excess length effects when stranded, and those with large amounts of excess lengths will show very much less effect than would be expected on the basis of the circular cross-section analysis.

The general case of an arbitrarily shaped distorted section can be handled for the condition that substantially all excess lengths are removed. Here, the final helix angle is nearly the same as the helix angle of the yarn before plying, since it can be shown that: $l_f = \frac{l_y}{\cos\theta_o}$ for the original yarn, and $l_f = \frac{l_y}{\cos\theta_f}$ for the final yarn, regardless of cross-section shape. The approximation involved will be discussed in a subsequent section when certain of the assumptions already made are examined. This case of complete excess length removal is of particular importance because a yarn will in general tend to distort until the excess lengths are removed, and while the entire yarn cannot be supposed to have reached this state, the deviations from complete removal of excess lengths will be largely for those fibers having low angles of inclination where the situation is not critical.

Calculation of strand efficiency should then make use of a yarn strength approximately that of the original yarns, or somewhat less for large amounts of untwisting in the plying process. Thus one cannot in general compute the translation of experimental yarn strength into strands or plied yarns

using data on yarn removed from plied or stranded structures, but must instead rely on the theoretical formulation.

The differences between rupture strength of a yarn as it lies in a strand and a yarn removed from a strand have now been partially accounted for, but any differences in the shapes of the stress-strain curve and the variation of elongation to break have not. Thus, the factor $m = b\sigma$ upon which the effects of variability are based, is not determined. Unfortunately, there is no unequivocal means of obtaining a value which can be considered accurate. It is probable that b, the stiffness, increases slightly from the value obtained for yarns removed from strands, but what happens to σ cannot be predicted. However, the value of $b\sigma$ for a given set of similar yarns, initially the same but with different amounts of twist removed by stranding or plying, does not vary very much, so it is reasonable to assume that the value of m for yarns in strands is close to the value for yarns removed from strands. Also, reference to Figure (10) will show that even a fairly large error in m will introduce only a few per cent error in the final efficiency.

The final point to be considered is the assumption that yarns support negligible load after attaining maximum load. The best proof of a clean-cut yarn rupture is obtained by observing a strand break. When a yarn snaps it appears to go almost completely. From the analysis given in Appendix I it can be seen that unless the broken yarn carried an appreciable load up to an extension well beyond its own breaking extension, there would be little effect on strand efficiency.

The first practical case to be considered is that of two three-ply Sansevieria ropes, one burnished and the other rough. These are small size ropes, the nominal weight of the singles in each being 380 feet per pound or 36,000 denier. Pertinent fiber and original yarn data for these structures has already been reported in Technical Report Number 6. In order to calculate the theoretical efficiency of the three-ply rope, the following data must be known:

1.) External helix angle of original yarn.

2.) Helix angle of the plied yarn, or rope in this case, initially and at rupture.

3.) Fiber properties.

   a. e_m, mean fiber rupture elongation, per cent.
   b. a/b, the ratio of load intercept to slope of the linear approximation to the average fiber stress-strain curve.
   c. V, the coefficient of variation of fiber elongation to rupture.

4.) b and σ for the yarn, theoretically as it lies in the final rope.

Using the yarn helix angle and the fiber properties, the singles yarn efficiency can be found from the curves given in Technical Report Number 6. The twist takeup of the yarn is found from the initial helix angle, as also given in Technical Report Number 6. The translational factor, μ, due to yarn variability is found from the curves of Figure (10) using a value of m equal to $b\sigma$ for the yarn. The twist takeup factor for the three-ply rope is given by the cosine of the initial ply angle, and the axial component of force by the cosine of the ply angle at rupture. Usually the initial and rupture ply helix angles will be sufficiently close so that there need be no differentration between them, but in this case the rope diameter decreased and length increased considerably as the specimen approached rupture so that a slightly better value is obtained by taking the change in angle into account.

In Figure (16) is given the average yarn stress-strain curve for yarns removed from the rough rope. The slope b is determined by the best straight line through the region of the curve near the average rupture point.

Table V gives all parameters and the theoretical results for the three-ply rough rope compared with experimental results.

TABLE V

PARAMETERS AND EFFICIENCIES FOR THREE-PLY SANSEVIERIA ROPE, ROUGH

Yarn Properties	
Single yarn efficiency, %	55.5%
b = slope to yarn stress-strain curve, % of ultimate load per per cent elongation.	41.6
σ = standard deviation of rupture elongation, %.	0.30
m = $b\sigma$	12.5
μ = yarn variability factor.	0.90
Rope Helix Angles	
$\cos \theta_{po}$ = cosine of original helix angle.	0.898
$\cos \theta_{pf}$ = cosine of helix angle at rupture.	0.929
Efficiencies of Three-ply Rope	
Theoretical	41.6 %
Experimental	40.8±3%

FIGURE 16

AVERAGE STRESS-STRAIN CURVE,
SANSEVIERIA YARNS, ROUGH

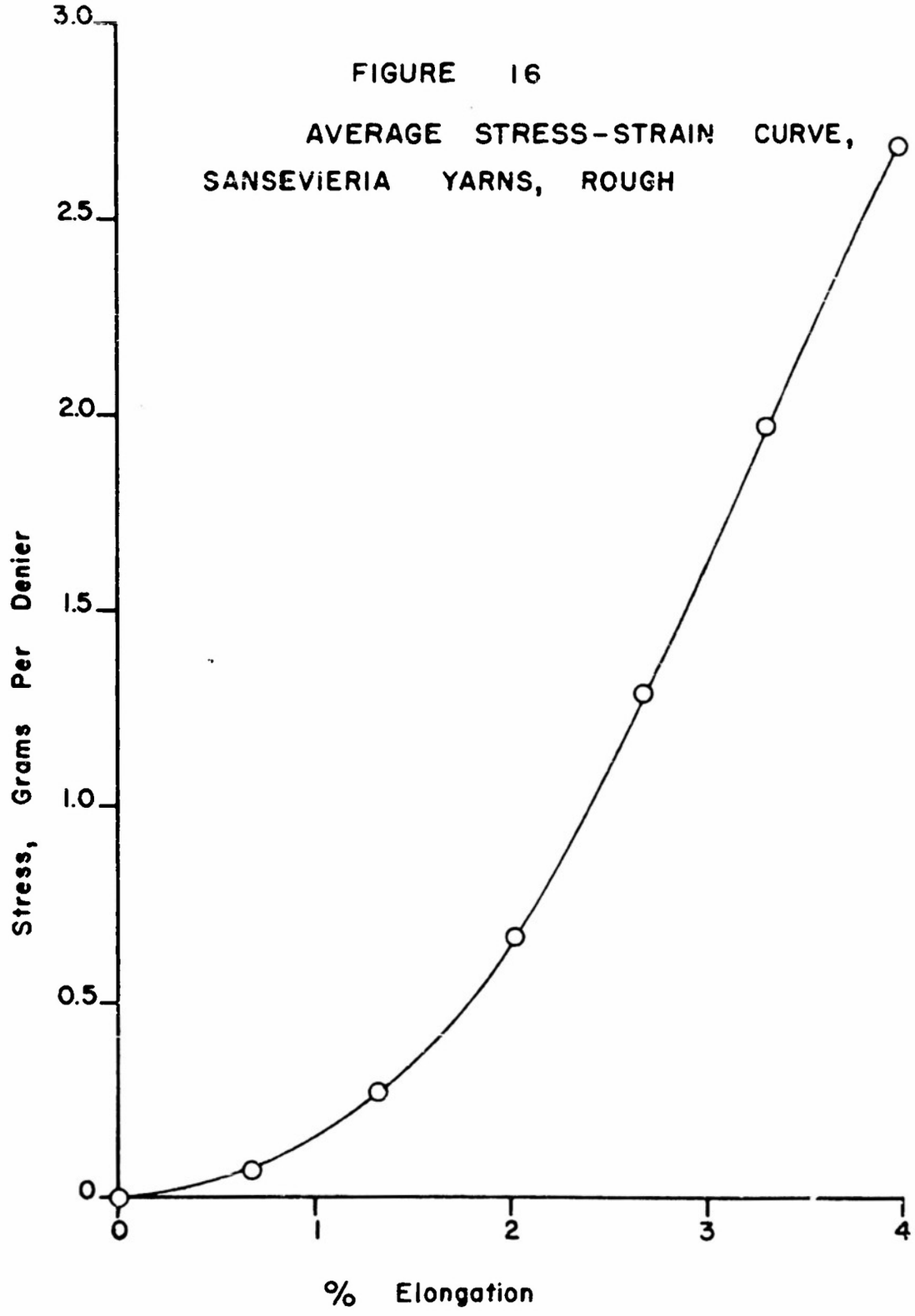

In Table V, μ is yarn variability factor as given by the curves of Figure (10), and cos θ_{po} is the rope twist takeup factor. As can readily be seen, the agreement between theoretical and experimental efficiencies is excellent, the differences being approximately 2%. It is to be noted that the combined effects of yarn variability and rope helix angles have accounted for an equivalent loss of yarn tenacity of the order of 25%, i.e., the translation of yarn strength to rope strength is about 75%. Thus, it is apparent that the major cause of the loss of nearly 60% of the fiber strength in this rope is the poor efficiency of translation of the fiber strength into the yarns. This latter is, as already described, the result of both nonuniformity of rupture extensibility among the natural Sansevivieria fibers and also their low average extensibility. No extensive tests were performed on the burnished rope, since it was indicated by gross screening that burnishing did not significantly effect the three-ply rope efficiencies. Thus, the burnished rope had an experimental efficiency of 42.9%±3 versus 40.8%±3 for the rough, the differences not being statistically significant. Experimental efficiencies of yarns removed from the three-ply ropes were 54.5% for the burnished and 53.5% for the rough ropes. Without consideration of excess fiber lengths each of these yarns would have given experimental efficiencies of 58.5%. While no formal analysis of excess lengths effects were made here, it was apparent from the method of rope formation that the effects would be small since in roping a partial compensation was made for twist removal, and hence the magnitude of excess lengths are small. In addition, the inherent variability of the Sansevieria fiber in these yarns is greater than that of the Manila abaca fiber (2) for which excess length effects were calculated in Table II. Thus, the higher variability of the Sansevieria fiber would mask the effect of excess lengths to below that of the abaca fiber, and an excess length effect for the former fiber of approximately the 10% experimentally observed is reasonable.

The next case to be considered is that of the series of Manila abaca strands made up of the yarns whose twist structure and strengths were considered in Tables (I and II). The approach is the same as that just considered for the Sansevieria ropes with one exception. It will be noted in the derivation of seven-ply yarn strength as given in Appendix III that the statistical effects cannot be completely separated from the geometric effects, and thus the exact analysis of the problem is rather complex. Strictly speaking analysis similar to that of the seven-ply structure applies to any case in which the constituent elements of the structure do not undergo equal strains as a result of a structure strain. Nonetheless, it can be shown that negligible error is introduced in the case of the 14 or 15 yarn strands if all 14 or 15 units are considered to be equally strained instead of having a more highly strained core yarn as is actually the case.

To show this consider the case of the seven-ply yarn in two ways:

a. efficiencies, η_1 calculated according to the previous rigorous analysis whose results are plotted in Figure (11).
b. efficiencies, η_2 calculated under the assumption of all seven units being at the same angle and thus supporting equal strains.

Table (VI) below gives the results for several cases.

TABLE VI

COMPARISON OF THEORETICAL SEVEN-PLY YARN EFFICIENCIES

θ	a/b	e_m	V	η_1	η_2
20°	-1	3	0	80.5	93.9
30°				75.0	86.6
20°	-1	3	5	79.5	84.5
30°				70.0	77.8
20°	-1	3	10	76.5	74.9
30°				66.0	69.0
20°	0	any value	0	85.4	93.9
30°				75.0	86.6
20°	0	any value	5	86.0	87.6
30°				71.3	80.7
20°	0	any value	10	81.0	81.3
30°				70.6	74.9
20°	1	3	0	87.6	93.9
30°				75.0	86.6
20°	1	3	5	89.5	89.2
30°				75.0	82.2
20°	1	3	10	83.1	84.4
30°				71.3	77.8

It can be seen that for any appreciable yarn variability, the values of η_1 and η_2 for a seven-ply yarn are sufficiently close so that the less extreme case of 14 or 15 units with a core would produce negligible differences whether considered as a parallel bundle or as a core and sheath configuration. The discrepancy is obviously less at small ply helix angles. In no case was a higher ply helix angle than 28° found for the Manila strands, whose average yarn rupture elongation variability was of the order of 10%. Clearly, the assumption of the strand structure containing all units in parallel would involve an error considerably less than the errors shown in Table (VI) for angles between 20° and 30° and for yarn variability of 10%. Thus, errors in efficiency of less than 1% would result from this approximation of strand geometry.

Table (VII) summarizes all of the pertinent information on structure and efficiencies of the abaca strands. Three values of efficiency are included for each strand; a.) theoretical efficiency without considering excess lengths; b.) theoretical efficiency considering full excess lengths; and c.) experimental efficiencies. Singles yarn efficiencies for the no excess length case are taken from Technical Report Number 6 and for the full excess length case from Table (II) of this report. It would be supposed that the experimental results would always fall somewhere between the theoretical predictions based on full excess and those based on no excess lengths. For small twist differentials, i.e., small amounts of singles untwisting, there should be a tendency for experimental values to approach the no excess length values since there are only small excess lengths to takeup. For large twist differentials better agreement should occur with the full excess length values. The full excess length values should be most closely approached where the final yarn twist is very small so that a great distortion would be necessary to restore the original angle and thus remove all excess lengths.

With the exception of one value, the following Table (VII) demonstrates these observations quite closely. In most cases, theoretical efficiency calculated without excess lengths are well within experimental efficiency ranges. The only value outside of the experimental range is that for SMM, and even here the error is small, being only 9% or 3.8 units of efficiency from the lower of the experimental limits. No explanation is apparent for the high experimental efficiency of SMM, but in view of the good agreement between experimental and theoretical values of efficiency for the other cases, it seems probable that some uncontrolled factor such as a yarn or fiber not representative of the variables considered is responsible.

Figures (17)-(20) illustrate the combined effects of fiber characteristics, singles twist, and ply twist in a form which may sometimes be useful. Each curve is for a given set of fiber parameters and shows the effect on efficiency of varying combinations of yarn and ply twist under the assumption of no excess lengths and no variation amongst yarns. The convention employed is that all points on a given curve correspond to a constant sum $(N_p + N_{yp})R_y$, where N_p is the ply twist in turns per unit length, N_{yp} is the number of turns per unit length of the yarn as it lies in the ply, and R_y is the singles yarn radius. The abscissa is given in terms of N_pR_y and thus the yarn parameter $N_{yp}R_y$ for any point on the curve is given by the value of $(N_p+N_{yp})R_y$ for the given curve minus the value of N_pR_y. The curves were plotted by converting the various NR values to helix angles and using the yarn efficiency curves given in Technical Report Number 6. In dealing with the case of yarn where excess lengths might be supposed to have been created in the plying process, the curves are still applicable if the excess lengths are assumed to have been taken up. In this case the $N_{yp}R_y$ to be chosen is that of the original yarn and not the yarn as it lies in the ply. This is in conformity with the preceding analysis wherein it was shown that the helix angle of a fiber whose excess length has been taken up by distortion must be very nearly equal to the angle of the fiber before any excess lengths were introduced, that is, before plying. In utlilizing these curves, the only additional factors to be employed for plied yarn efficiency calculations are:

a.) Twist takeup of original singles yarns.
b.) Plied yarn twist takeup.
c.) The yarn variability factor, μ, as given by the curves of Figure (10).

TABLE VII

COMPARISON OF THEORETICAL AND EXPERIMENTAL STRAND EFFICIENCIES

Strand Code	Single Yarn Efficiency, % No Excess Lengths	Single Yarn Efficiency, % Full Excess Lengths	Yarn Variability Parameters m	Yarn Variability Parameters μ	Cosine Strand Helix Angle	Strand Efficiencies, % No Excess Lengths	Strand Efficiencies, % Full Excess Lengths	Strand Efficiencies, % Experimental
SSS	58.8	54.0	11.6	0.80	.931	40.7	37.4	41.4±2
SSM	58.8	53.2	15.0	0.75	.897	35.5	32.1	37.1±3
SSH	58.8	51.2	15.1	0.75	.880	34.3	29.8	31.0±2
SMS	56.3	49.5	14.3	0.76	.945	38.3	33.6	40.6±3
SMM	56.3	47.0	12.0	0.79	.917	37.7	31.2	43.5±2
SMH	56.3	45.2	14.1	0.76	.878	33.1	26.6	29.6±2.5
SHS	52.5	47.8	15.3	0.74	.943	34.6	31.4	31.8±2
SHM	52.5	47.8	15.3	0.74	.942	34.5	31.4	33.2±5.5
SHH	52.5	47.8	15.3	0.74	.931	33.7	30.7	33.4±6

FIGURE 17

THEORETICAL PLIED YARN EFFICIENCY

Yarn Rupture Elongation Variability = 0

Fiber Properties:

V = 0

a/b = 0

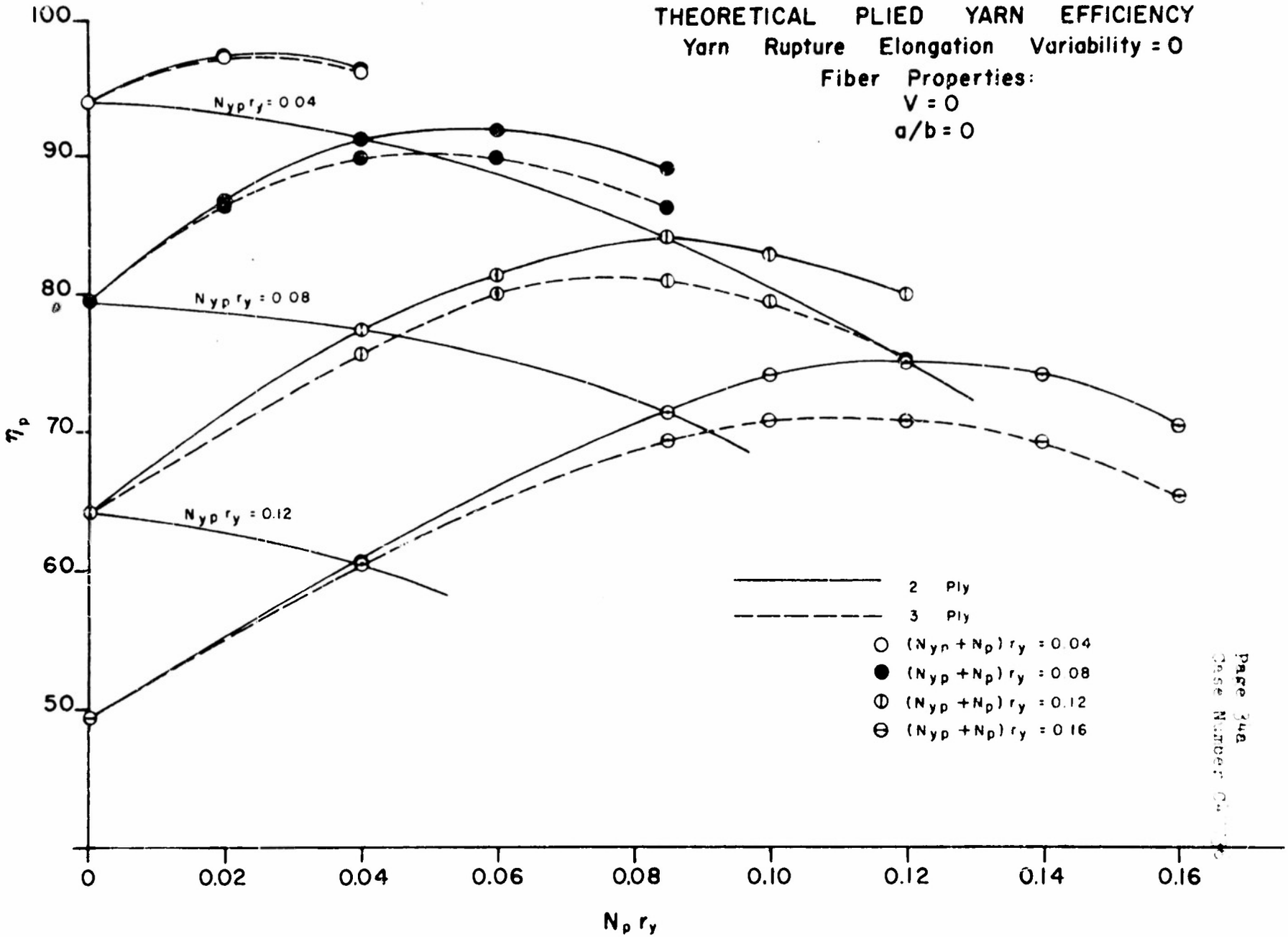

FIGURE 18

THEORETICAL 3-PLY YARN EFFICIENCY

Yarn Rupture Elongation Variability = 0

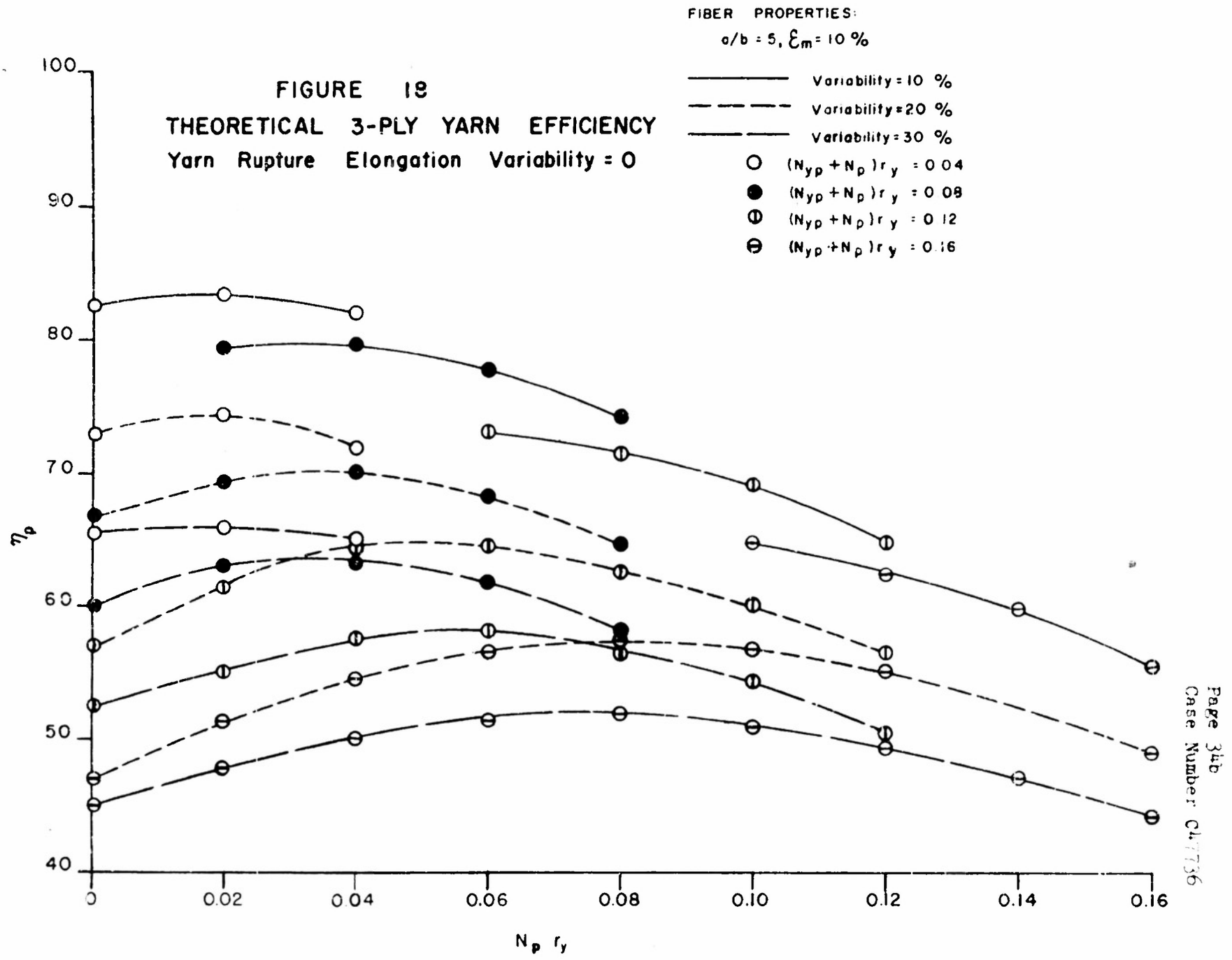

FIGURE 19

THEORETICAL 3-PLY YARN EFFICIENCY
Yarn Rupture Elongation Variability = 0

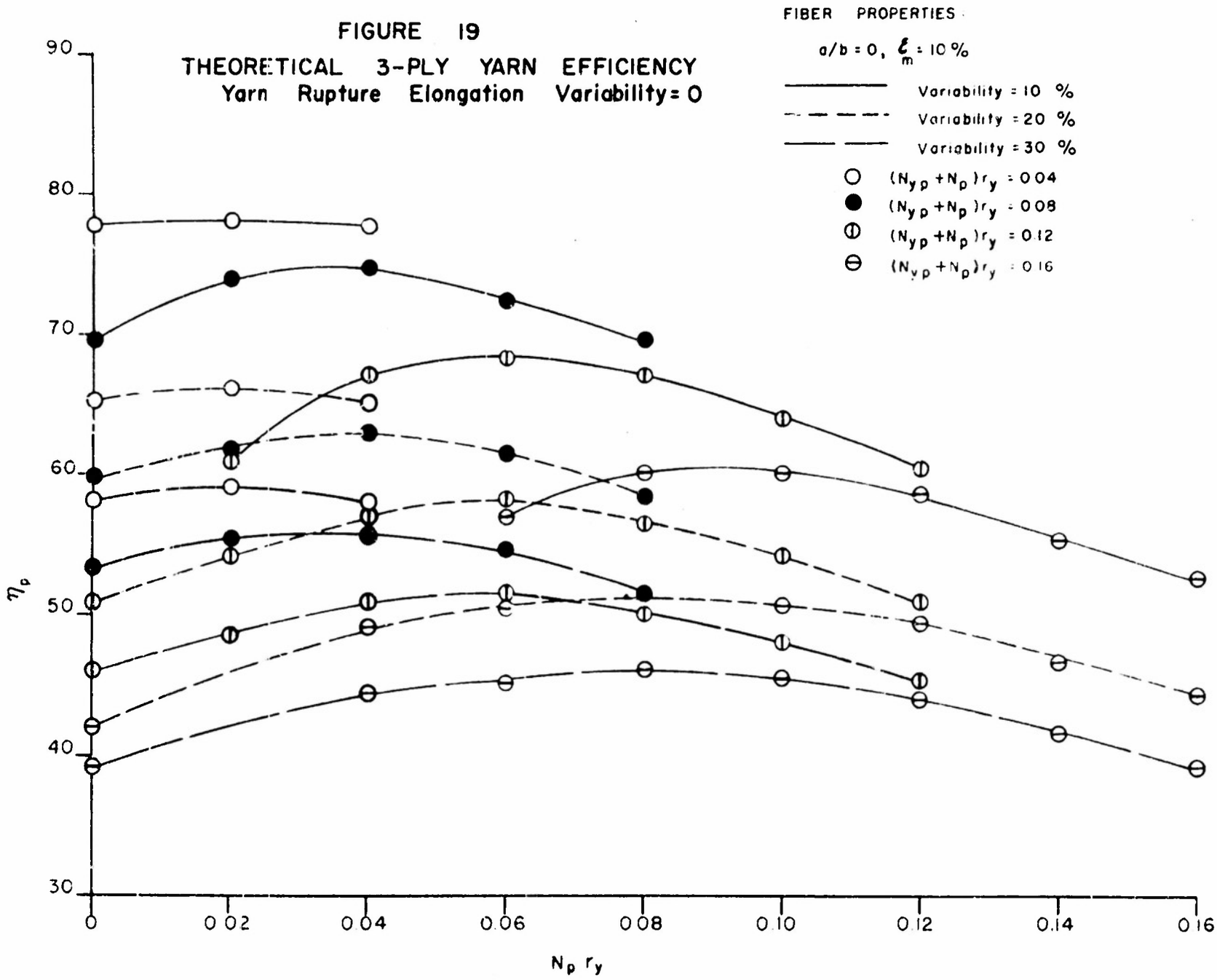

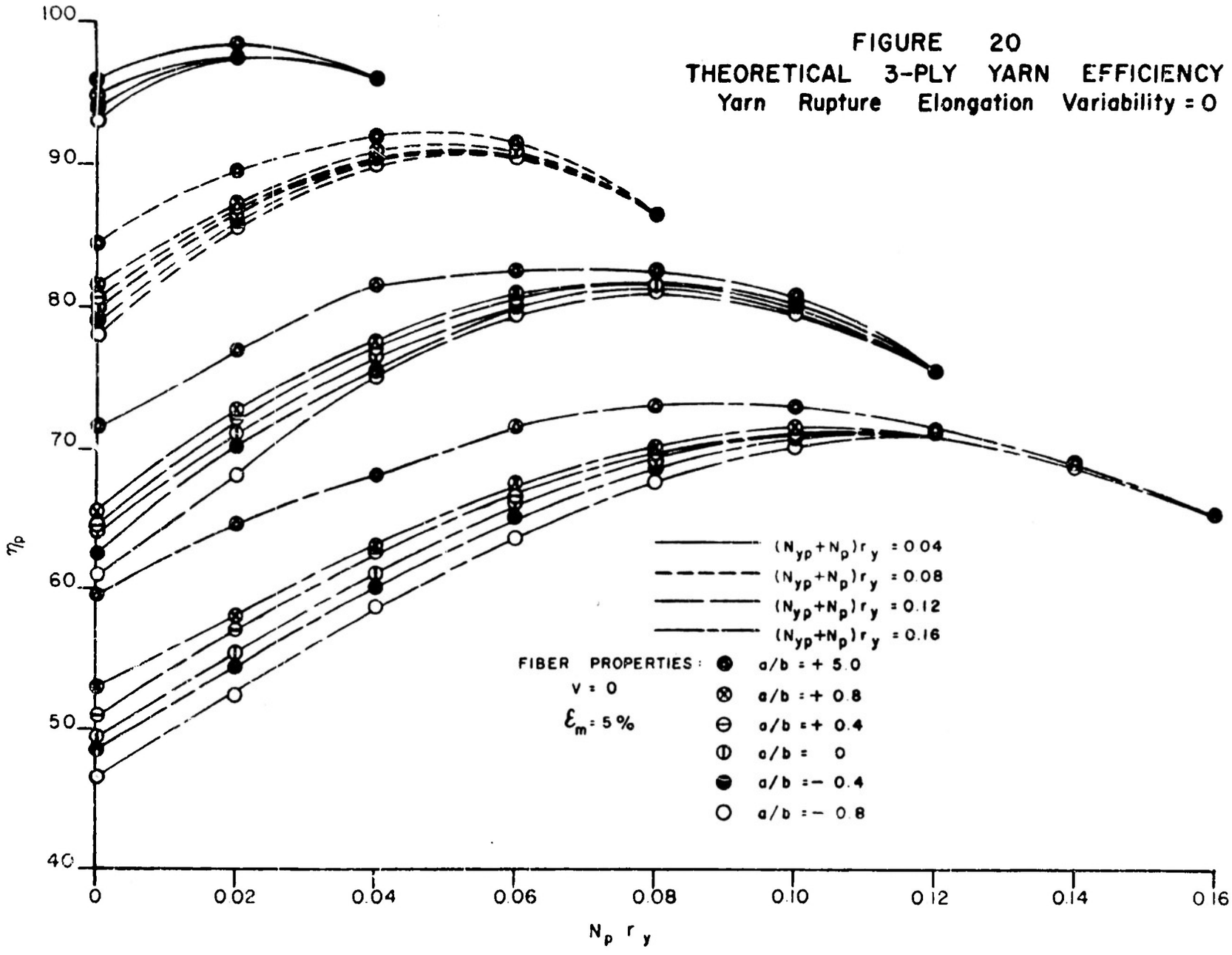

FIGURE 20
THEORETICAL 3-PLY YARN EFFICIENCY
Yarn Rupture Elongation Variability = 0

IV. DISCUSSION

A. Geometric Assumptions

Throughout the foregoing analyses, several simplifying geometric assumptions have been made to facilitate the mathematical solution of the problem. The results so obtained differ negligibly from those that would be obtained by employing a more rigorous geometric analysis, for structures which are of commercial interest. Portions of the geometrical problem involved here have been analysed quite rigorously by Chow (5). The geometric results of Chow's work are theoretically valid over a range of helix angles in excess of that required for the present problem. In the comparison which follows it will be shown that:

a.) The two approaches yield negligibly different results over the practical range of singles, strand, and rope twists, and

b.) Where the results do diverge appreciably, the assumptions involved in either analysis with respect to cross-sectional circularity are strongly violated.

Thus it is not expected that the more involved approach would produce more useful or realistic results, and the comparison is made only to show the order of magnitude of possible errors due to the simplification, and thus justify the exclusion of tortuous twist, as such, from the analysis.

1.) Comparison of Helix Angles

In the simplified approach, it has been assumed that the helix angle of the path of a fiber in a singles yarn as it lies in a plied yarn or strand can be determined from:

$$\tan \theta_{yp} = 2\pi R_y H_{yp}$$

where θ_{yp} is the fiber helix angle of the singles as it lies in the ply or strand, R_y is the radius of the singles yarn, and H_{yp} is the turns of twist per unit length of the singles as it lies in the ply. According to Chow's work:

$$\tan \psi = \frac{2\pi R_y \left(H_{yo} - H_p \cos^2 \theta_p \right)}{1 - \frac{R_y}{R_p} \sin^2 \theta_p \cos \phi} \qquad \text{(25)}$$

where:

ψ is the angle between the fiber and the singles yarn axes; N_{yo} is defined as the twist per unit length a singles yarn would have if it were removed from the ply in accordance with the procedure of Figure (4a); N_p is the ply twist per unit length; R_p is the radial distance from the plied yarn center to a singles yarn center; and ϕ the position angle which locates a fiber in the singles cross-section, equal to zero at the inside of the bend of the singles yarn.

The expression for θ_{yp} can be put into the form of Equation (25) by realizing that the pure twisting procedure of Figure (4a) will remove $N_p \cos \theta_p$ turns per unit length from the sirgles. Thus:

$$\tan \theta_{yp} = 2\pi R_y \left(N_{yo} - N_p \cos \theta_p\right) \qquad (26)$$

The value of ψ depends slightly on the position angle, ϕ, but the denominator of Equation (25) has an average value very nearly equal to unity, so that the average value of tan ψ can be taken to be:

$$\overline{(\tan \psi)} = 2\pi R_y \left(N_{yo} - N_p \cos^2 \theta_p\right) \qquad (27)$$

The two angles $\overline{\psi}$ and θ_{yp} can also be conveniently expressed as:

$$\tan \theta_{yp} = \tan \theta_o - \frac{R_y}{R_p} \tan \theta_p \cos \theta_p$$

$$\tan \left(\overline{\psi}\right) \doteq \overline{(\tan \psi)} = \tan \theta_o - \frac{R_y}{R_p} \tan \theta_p \cos^2 \theta_p \qquad (28)$$

To show the magnitude of the difference between θ_{yp} and $\overline{\psi}$ some values for a few different sets of condition have been compiled in Table VIII.

TABLE VIII

COMPARISON OF HELIX ANGLES $\overline{\psi}$ AND θ_{yp}

a.) $\frac{R_y}{R_p} = 1$ (2 ply yarn)

	Values of $\overline{\psi}$ for:			
θ_p	$\theta_{yp} = 5°$	$\theta_{yp} = 10°$	$\theta_{yp} = 20°$	$\theta_{yp} = 30°$
5°	5°	10°	20°	30°
10	5.1	10	20.2	30
15	5.5	10.5	20.4	30.4
20	6.2	11.1	21.0	30.8
25	7.2	12.2	22.0	31.7
30	8.8	13.6	23.3	32.7

TABLE VIII (continued)

COMPARISON OF HELIX ANGLES $\overline{\psi}$ AND θ_{yp}

b.) $\frac{R_y}{R_p} = 1/2$ (7 ply yarn)

	Values of $\overline{\psi}$ for:			
θ_p	$\theta_{yp} = 5°$	$\theta_{yp} = 10°$	$\theta_{yp} = 20°$	$\theta_{yp} = 30°$
20°	5.5	----	----	30.4
30°	6.8	----	----	31.4

Clearly the differences between the two methods are nowhere large, and, in addition, the maximum angular differences occur at the low values of $\overline{\psi}$ or θ_{yp} where differences are of small importance. The differences also decrease as θ_p and $\frac{R_y}{R_p}$ decrease. $\frac{R_y}{R_p} = 1$ is the condition for a two ply yarn, while $\frac{R_y}{R_p} = 1/2$ represents the outer layer of a seven ply yarn. The local value of ψ is slightly changed by the denominator given in Equation (25). However, the effect on strength of such a change would be slight unless θ_p were quite large i.e., greater than 30°. This is most easily understood if it is recognized that for most of the fibers in the entire singles yarn cross-section, differences between ψ and $\overline{\psi}$ are negligible.

2.) Comparison of Excess Lengths

When the helix angle of a yarn is lowered by virtue of partial untwisting, the required helical path length is decreased, but the actual fiber length remains unchanged, giving rise to excess fiber lengths. In this report the required path length of a fiber in a plied yarn per unit length of the plied yarn has been taken to be:

$$\ell_f = \frac{1}{\cos \theta_p} \sqrt{1 + \tan^2 \theta_{yp}} \qquad \text{---------- (29)}$$

while Chow's work yields, for a ϕ interval of $2\pi N$, where N is any integer, i.e., for an integral number of fiber cycles:

$$\ell'_f = \frac{1}{\cos \theta_p} \sqrt{1 + \tan^2 \overline{\psi}} \qquad \text{---------- (30)}$$

In either case the original fiber path length is the same, being simply that length corresponding to the original singles helix angle. In Table (IX) a comparison is made of excess lengths for a wide range of singles and plied yarn twists as determined from both Equations (29) and (30).

TABLE IX

COMPARISON OF EXCESS LENGTHS ℓ_e AND ℓ'_e

a.) $\frac{R_y}{R_p} = 1$, $\theta_p = 30°$

Original Single Helix Angle, θ_o	θ_{1p}	$\overline{\psi}$	ℓ_e	ℓ'_e
45.3°	27.2°	30°	21.0%	19.0%
30.5	5.0	8.8	13.4	12.8
26.5	0.0	3.8	10.7	10.5

b.) $\frac{R_y}{R_p} = 1$, $\theta_p = 20°$

42.6°	30°	30.8°	14.0%	13.2%
27.4	10	11.1	10.1	9.7
23.2	5	6.2	7.9	7.7
18.9	0	1.2	4.8	4.7

c.) $\frac{R_y}{R_p} = 1$, $\theta_p = 15°$

24°	10.5°	11°	7.1%	7.0%

d.) $\frac{R_y}{R_p} = 1$, $\theta_p = 10°$

30°	21.9°	22.1°	6.5%	6.3%
20	10.8	10.9	4.5	4.5
15	5.0	5.0	2.9	2.9
10	0.0	0.1	1.5	1.5

e.) $\frac{R_y}{R_p} = 1/2.\ \theta_p = 15$

24°	17.6°	17.8°	5.1%	5.1%

Over the range of ply and singles helix angles covered, which it is believed encompasses the practical range, it is clear that differences in calculated excess lengths are small, with Chow's formula always yielding the slightly smaller value.

It should be noted that calculations of fiber length and strains involve an integration over ϕ from 0 to 2π. This is an impossible procedure if $\theta_o = 0$, for here a given fiber remains at the same angle ϕ throughout its length, and thus this situation represents a point of discontinuity in the equations relating to length. However, the matter is of no practical importance since $\theta_o = 0$ is equivalent to plying zero twist bundles. It is doubtful whether such a procedure could be made to yield a structure whose original elements remained separate and distinct, much less circular.

3.) Comparison of Fiber Strains

Fiber strains may be compared on both an average and local basis, just as angles. In the work of this report only the average fiber strain has been used and it has been taken to be:

$$e_f = e_p \cos^2\theta_p \cos^2\theta_{yp} \qquad \text{(31)}$$

where e_p is the strain along the plied yarn axis. Here again the secondary effects of tortusoity have been neglected and the singles yarn is considered to have essentially the same geometric properties as if it were removed from the plied yarn and retained its twist as it lay in the ply.

Based upon Chow's analysis, the following expression for the average strain in one complete loop of fiber as it lies in a plied yarn can be derived:

$$e_f' = \sqrt{\frac{(1+e_p)^2 + \tan^2\theta_p}{1 + \tan^2\theta_p}} \cdot \frac{\sqrt{1+\left[\dfrac{\tan\theta_o}{1+e_p\cos^2\theta_p} - \dfrac{R_y}{R_p}\dfrac{(1+e_p)\tan\theta_p}{(1+e_p)^2+\tan^2\theta_p}\right]^2}}{\sqrt{1+\left[\tan\theta - \dfrac{R_y}{R_p}\dfrac{\tan\theta_p}{1+\tan^2\theta_p}\right]^2}} - 1 \qquad \text{(32)}$$

In Table (X) the results of Equations (31) and (32) are compared. An additional comparison is made in some cases where the simplified formula, Equation (31), used in this report is employed, but $\overline{\psi}$ is substituted for θ_{yp}. This value of strain is labelled e_f''.

TABLE X

COMPARISON OF STRAINS COMPUTED FROM EQUATIONS 31 AND 32

θ_p	θ_o	e_p	$\frac{R_y}{R_y}$	Eq. (31) e_f	Eq. (32) e_f'	Eq. (31) with $\theta_{yp} = \overline{\psi}$ e_f''
25°	30°	0.02	1	0.0160	0.0156	------
25	42	0.02	1	0.0134	0.0125	0.129
25	42	0.10	1	0.067	0.064	0.064
15	23	0.02	1	0.0182	0.0181	------
15	36	0.02	1	0.0153	0.0151	------
25	42	0.10	1/2	0.056	0.052	0.054
25	34	0.02	1/2	0.0135	0.0131	0.0133
25	34	0.10	1/2	0.068	0.067	0.067

The differences between e_f and e_f' are small anywhere within the range tabulated. It can be seen that the differences tend to become larger as θ_p or $\frac{R_y}{R_p}$ increase, but $\frac{R_y}{R_p}$ cannot exceed unity. A large part of the difference between e_f and e_f' can be ascribed to the difference between θ_{yp} and $\overline{\psi}$, as is evidenced by the relative closeness of e_f' and e_f''.

From Chow's work it is also possible to determine the magnitude of the local fiber strain still, of course, under the assumption of circularity of yarn cross-sections. The results, for an extreme case, are given below in Table (XI).

TABLE XI

LOCAL FIBER STRAINS FOR A PLIED YARN STRUCTURE

$\frac{R_y}{R_p} = 1$, $\theta_p = 30°$, $\theta_o = 30°$, $e_p = 0.10$.

ϕ	Local Strain, e_f, ϕ
0	11.5
$\frac{\pi}{2}$	7.0
π	4.7
Average	7.5
$e_p \cos^2\theta_p \cos^2\theta_{yp}$	7.5

The above Table (XI) would seem to show that very great stress differentials exist between the various portions of a given fiber, depending upon its position angle ϕ. However, a number of factors tend to mitigite the severity of local conditions as shown by this analysis: 1.) If local differences in strain are admitted, then local differences in excess length must also be considered, and the high excess length regions occur just when high strain would be predicted, i.e., at $\phi = 0$; 2.) Any freedom of motion of fibers whatsoever would tend to equalize strains, and some freedom of motion must exist; 3.) It has been demonstrated earlier in the report that any distortion of the yarn from circularity will tend to remove excess lengths, and by a direct extension of this reasoning it is easy to see that unequal strains along the length of a given fiber will cause an equalizing distortion. These distortions can occur either before or during the loading of the structure or at both times. As stated previously, distortions before loading can occur as the result of the presence of excess lengths. Such distortions tend to alter the local fiber radii of curvature considerably from that for circular yarns. The local strains given in Table (XI) are critically dependent upon local radii of curvature, whereas the average strains are not so dependent. Examples of distortion under loading, for a circular cross-section yarn with no excess lengths, would be: (a) local flattening in the region of high fiber strain; (b) higher freedom of fiber relative motion in the region of low fiber strain with the attendent opportunity of fiber length travel to the region of high fiber strain. Both mechanisms will equalize fiber strain. Thus differences in local strain may safely be considered negligible and the average values used. It is also clear from the experimental strength and rupture elongation results that large differences in strains do not exist, since large differences would produce much lower strand and rope efficiencies and elongations than those observed.

It is apparent from the foregoing that for circular yarn cross-sections, the simplified geometric relations assumed and used in the body of this report differ inappreciably in most cases from the average geometric relationships obtained by Chow. The difficulty of comparing local geometric and strain discrepancies has already been discussed, and it has been indicated that local strains and stresses must approach the average when plied yarns are stressed. Nevertheless, it is also evident that with increases in ply or strand helix angles very greatly in excess of 30°, increasing discrepancies arise between the average rigorously derived geometry and the simplified geometry used herein. These discrepancies are in the direction of lowering the plied yarn strength, i.e., lower plied yarn or strand efficiencies would be given using Chow's geometry than those given by the simplified geometry* While great cross-sectional distortion will usually take place for such high ply or strand helix angles, it is conceivable that some extreme structures may be encountered which will be weaker than the calculations in the body of this report indicate. For such structures, calculations based upon Chow's geometric analysis would determine one limit of efficiency while the other limit would be determined by the formulae given herein. Cross-sectional distortion would then produce a final result somewhere between the two extreme limits. Clearly, the structures studied in this report are performing under tension in a manner consistent with either

---

*Assuming no excess lengths.

Chow's average or the simplified geometry. Since these structures cover as broad a range of commercial cordage twists as is feasible, it is clear that they encompass substantially all cordage structures of interest.

B. Application to Higher Order Structures

Technical Report Number 6 and the present work have covered what appear to be the most significant factors affecting the translation of strength of fibers into practical singles yarns, plied yarns, and strands, with emphasis on cordage materials. It is possible to apply this work directly to higher order structures, such as ropes, simply by interchanging the roles of rope and strand, and strand and yarn. Thus the rope is treated as a strand composed of yarns which are in reality strands, and whose properties are known. The only additional assumption involved is that strand rupture is complete after maximum strand load is attained. Observations of rope breaks tend to indicate this to be reasonable. Unfortunately, complete sets of data on rope, covering fiber, yarn, and strand properties and rope breaking strength are not available, but from the scanty data which is at hand, it appears that the above projection yields good results.

APPENDIX I

Analysis of Parallel Bundle Strength

A parallel bundle, in this work, is used to refer to a group of units each of which is supporting equal strains as a result of straining the entire group. Thus, a three-ply yarn contains three units (singles yarns) in parallel. The equal strains would, in the case, of a three-ply yarn, be less than the strain applied to the three-ply because of the ply helix angle. However, this latter effect is geometrical, and merely requires geometric factors to be applied following the analysis of the statistical effect on three yarns in parallel with zero ply helix angle. It is the statistical analysis which follows.

Consider a population of units with normal distribution of elongations to break and a given average load elongation diagram (Figure 21a and 21b). The abscissae are normalized to the statistical t, or number of standard deviations from the mean elongation.

If there are n of the above units in a bundle, there exist the possibilities that maximum load is reached when the first unit breaks, or when the second unit breaks, and so on, to the nth unit. Clearly if n = 2 there is a very low probability for ever attaining a higher load than that reached when the first unit broke (except in cases of very high variability). Conversely, if n is very large, say 100, the maximum bundle load will almost certainly not be reached until several units have ruptured. The factors defining attainment of maximum load will now be formulated analytically.

Assume the first of the n units to break at an elongation corresponding to t_1 and specify that the maximum load shall be attained at this point. The load supported by the bundle here is $ng(t_1)$. In order that this be the maximum bundle load it follows that the load on the bundle when the second unit breaks, where there are only (n-1) units intact, shall be less than $ng(t_1)$. In the limiting case of equal loads at both first and second unit failure, $(n-1)\,g(t_2) = ng(t_1)$. Similarly for the third unit rupture, when n-2 units are intact, $(n-2)\,g(t_3) = ng(t_1)$, for maximum load to occur when the first unit breaks, etc. Thus the second unit must rupture before the average load per unit is $g(t_2)$, where $g(t_2) = \frac{n}{n-1}\,g(t_1)$; the third before the average load per unit is $g(t_3)$, etc. The values of t_i can be found from the load elongation diagram since $g(t_1)$ is known from the arbitrarily chosen first break point and the above equalities.

The above limiting equalities also hold when maximum strength is reached at other than the first break. It is necessary only to determine the strengths corresponding to the arbitrarily chosen value of t_1. Thus there are several distinct cases to solve: distributions of bundle loads which are maxima first unit breaks; maxima second breaks, and so on. All cases must be calculated which contribute any considerable portion to the total number of bundle breaks.

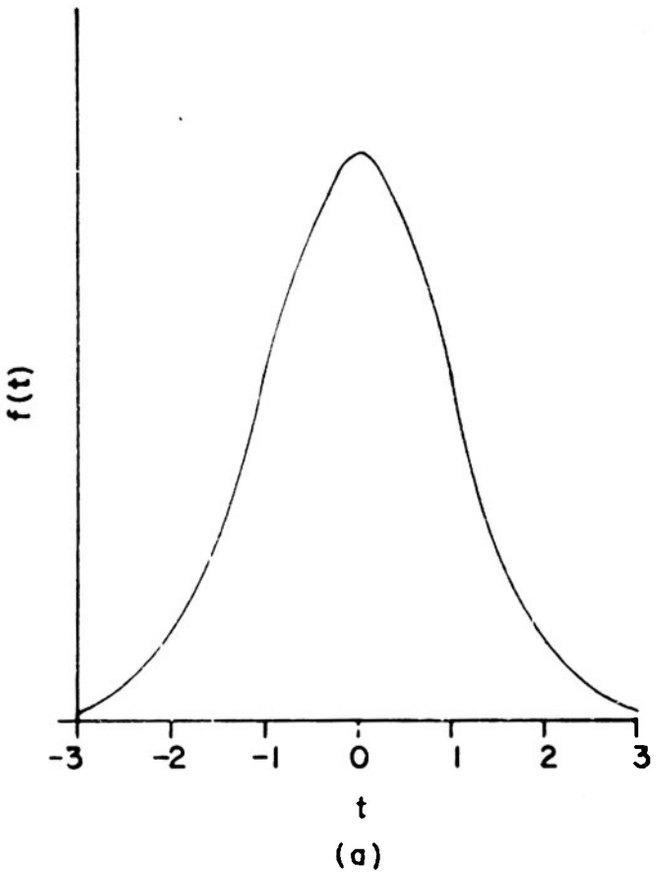

NORMAL DISTRIBUTION OF RUPTURE ELONGATION

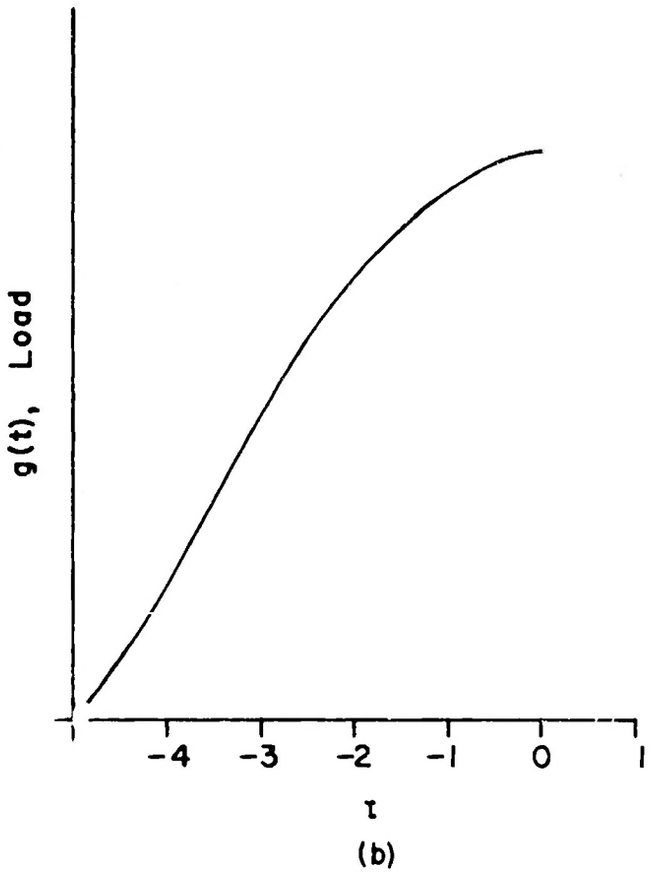

AVERAGE LOAD ELONGATION CURVE

FIGURE 21

The formulation of both the separate probabilities for the case of a maximum bundle load being reached when the first unit breaks, the second, etc., and also the efficiency in terms of the various influencing parameters will now be undertaken.

The following definitions apply to the analysis:

p_i = probability of any unit breaking at an elongation within the interval t_{i-1}, and t_i where $t_0 = -\infty$

$$= \int_{t_{i-1}}^{t_i} f(t)dt = \frac{1}{\sqrt{2\pi}} \int_{t_{i-1}}^{t_i} e^{\frac{-t^2}{2}} dt$$

(The probability integral in terms of t; values of this definite integral can be found in tables of areas under the normal curve.)

q_i = exponent of p_i factor in any term of the expansion below.

$h(t)_\ell$ = relative frequency of occurrence of a maximum bundle load at t when the ℓth unit breaks at t.

C = a normalizing constant such that the total probability will equal unity.

It is first desired to plot a curve of relative frequency of maximum bundle load versus t for the case of a maximum occurring where the first unit breaks, $h(t)_1$, when the second unit breaks, $h(t)_2$, etc. Consider for example, the determination of $h(t)_1$.

It is known from probability theory that if the probability of a given event occurring is p_1, another event p_2, etc., that in a total of n events, the probabilities of various combinations can be represented by the expansion of:

$$(p_1 + p_2 + \ldots\ldots\ldots p_n)^n \quad \text{---------- I-1}$$

The terms of this expansion will all be of the form:

$$A\, p_1^{q_1}\, p_2^{q_2} \ldots\ldots\ldots p_n^{q_n}$$

where A will have a value depending on the term, and:

$$\sum_{i=1}^{n} q_i = n \quad \text{---------- I-2}$$

In each term of the expansion the exponents q_i represent the number of occurrences of the event whose probability is p_i, while the whole term, including the coefficient, represents the probability of the combination of events designated by

the p_i's and q_i's. It is now necessary to formulate some method for rejecting all combinations which do not satisfy the prescribed conditions, in this case that a maximum is always reached when the first unit breaks. It has already been established that the second unit must break before reaching an elongation corresponding to t_2, the third before t_3, the fourth before t_4, etc. These conditions are satisfied, of course, if the second, third and fourth units all break before t_2, or if the second and third break before t_2 and the fourth before t_3, etc. The expression to be expanded is:

$$(p_2 + p_3 + \ldots\ldots p_n)^{n-1} \qquad \text{I-3}$$

It is obvious that the relative frequency of first unit breaks which produce maximum bundle loads at an elongation t_1 is the product of the relative frequency of any unit breaking at t_1 and the probability of the existence of a breaking array among the remaining units such that the first unit break at t_1 be a maximum.
Thus:

$$h(t)_1 = Cf(t_1) \quad (p_2 + p_3 + \ldots\ldots p_n)^{n-1}$$

$$\sum_{i=2}^{k} q_i \geq k - 1, \quad k = 2, 3, \ldots\ldots n \qquad \text{I-4}$$

The exponent is n-1 rather than n here since the breaking elongation of the first unit is arbitrarily specified, and the relative frequency of occurrence of this breaking elongation (t_1) is $f(t_1)$. The second of Equations I-4 specify the necessary and sufficient conditions such that each of the terms of the expansion I-3 satisfy the assumption of maximum bundle load being attained at first unit break. It is not obvious before beginning calculations how many terms of Equation I-3 must be considered for numerical accuracy, but clearly any very small value for p_i may be omitted from the calculations. Thus, the procedure used in determining the $h(t)_1$ curve involves:

a.) The selection of a series of arbitrary values of t_1 and the corresponding values of $f(t_1)$.
b.) For each value of t_1, so chosen the determination of the corresponding limiting values of $t_2 t_3$, etc., from the $g(t)$ equalities previously described.
c.) The determination of p_2, p_3 etc. for each value of t_1 and its corresponding t_2, t_3 etc., from the probability integral.
d.) The evaluation of the first of Equations I-4 retaining only those terms which satisfy the second of Equations I-4.

The curve $h(t)_1$ can be replotted as a curve of strength versus t_1, where strength is equal to the product of n, the total number of units in the bundle and the load per unit, $g(t_1)$. Thus, average bundle load of those first unit ruptures which produce maximum bundle loads is $n\,\overline{g(t_1)}$.

In an entirely analogous manner, all the values of $h(t)_\ell$ can be formulated with the following results:

$$h(t)_2 = Cf(t_2)\ (p_1 + p_3 + p_4 \ldots\ldots p_n)^{n-1} \qquad \text{I-5}$$

$$q_1 = 1;\ \sum_{i=3}^{k} q_i \geq k-2,\ k = 3,4,\ldots\ldots n$$

$$h(t)_3 = Cf(t_3)\ (p_1 + p_2 + p_4 + p_5 \ldots\ldots p_n)^{n-1} \qquad \text{I-6}$$

$$q_1 \neq 0,\ q_1 + q_2 = 2,\ \sum_{i=4}^{k} q_i \geq k-3,\ k = 4,5\ldots\ldots n$$

The results of the above can be replotted as curves of frequency versus bundle strength, the strength being given by the product of g(t) and the number of units intact when maximum bundle load is attained. For the case where a maximum is reached where the first unit breaks, the number of units intact is n; for a maximum when the second unit breaks, it is n-1; for the third, n-2, etc. Average maximum bundle loads are then given as $n\ \overline{g(t_1)}$; $(n-1)\ \overline{g(t_2)}$; $(n-2)\ \overline{g(t_3)}$, etc.

In previous work (1,2) a linear approximation to the stress-strain curve proved very useful for computational purposes. Here again, if a linear curve is used a great simplification results. Thus using the terminology of the previous work, the load supported by a unit can be expressed as a+be, or in terms of V, t, and e_m, $a+be_m\left(1+\frac{Vt}{100}\right)$, which is g(t). The assumption of a linear curve permits simplified analytical calculations rather than graphical, but all of the foregoing analysis still applies.

Once the several curves of frequency versus strength have been obtained for the various conditions for a maximum, it is necessary only to find the mean value of the abscissae of the curves weighted according to the number of units intact when maximum load is attained or:

$$\frac{\int_{-\infty}^{\infty} \sum_{\ell=1}^{n} h(t)_\ell \left[n-(\ell-1)\right]\left[a + be_m\left(1 + \frac{Vt}{100}\right)\right]dt}{n\int_{t=-\infty}^{\infty} \sum_{\ell=1}^{n} h(t)_\ell\ dt} \qquad \text{I-7}$$

Let:

$\bar{t}_1$ = mean value of elongation (in terms of t) of all those parallel bundle breaks which attain maximum load when the first unit ruptures.

$\bar{t}_2$ = mean value of elongation of all those parallel bundle breaks which attain maximum load when the second unit ruptures.

t_3 and t_4 are similarly defined.

For a linear load-elongation curve, the mean value of the loads corresponding to each of the above elongations is $g(\bar{t}_1)$, $g(\bar{t}_2)$ etc. Thus,

the corresponding total bundle loads are obviously: $ng(\bar{t}_1)$, $(n-1)\,g(\bar{t}_2)$, $(n-2)\,g(t_3)$ etc. The areas bounded by each of the curves, $h(t)\ell$, represent the relative number of all bundle breaks which produce maximum load at first unit break, second unit break, etc. Thus, the total number of bundle breaks is proportional to the sum of the areas, $(A_1 + A_2 + A_3 + \ldots\ldots A_n) = \sum_{n=1}^{n} A_n$ and the relative frequency of breaks which exhibit maximum load at first unit rupture is $\frac{A_1}{\sum_{n=1}^{n} A_n}$, second unit rupture $\frac{A_2}{\sum_{n=1}^{n} A_n}$, etc. Thus, the average value of maximum bundle loads for all bundle breaks is:

$$\bar{P}_B = \frac{A_1}{\sum_{n=1}^{n}(A_n)}\, n\, g(\bar{t}_1) + \frac{A_2}{\sum_{n=1}^{n}(A_n)}\,(n-1)\, g(\bar{t}_2) + \ldots\ldots\ldots \frac{A_n}{\sum_{n=1}^{n}(A_n)}\,(1)\, g(\bar{t}_n)$$

$$= \frac{1}{\sum_{n=1}^{n} A_n}\left[A_1 n\, g(\bar{t}_1) + A_2(n-1)\, g(\bar{t}_2) + \ldots\ldots A_n\, g(\bar{t}_n)\right] \text{ ---------- I-8}$$

The average bundle efficiency is then determined as the ratio of average maximum bundle load at rupture divided by the product of the number of units in the bundle, n, and the average breaking load of the units, $a+be_m$. Thus bundle efficiency is determined as:

$$\eta_B = \frac{A_1 n\, g(\bar{t}_1) + A_2(n-1)\, g(\bar{t}_2) + \ldots\ldots A_n g(\bar{t}_n)}{n(a+be_m) \sum_{n=1}^{n} A_n}$$

The values of $\bar{t}_1$, $\bar{t}_2$, etc. are determined by inspection of the individual distribution curves, $h(t)\ell$, which are substantially symmetrical.

While the foregoing relationships are general, the determination of specific values for: $\bar{t}_n$, A_n, and thus, efficiency, depends upon the particular bundle size, n, and the properties of the units which comprise the bundle, a, V, e_m. The curves given in Figure(10)are the results of calculations of a sufficient number of specific cases to permit simple determinations of bundle efficiency for a broad range of the variables. As indicated previously, the parameter $m = \frac{be_m V}{100}$ is used to characterize the properties of the units which comprise the bundle, where, in terms of previously defined parameters, $m = \frac{V}{\left(\frac{a}{be_m} + 1\right)}$.

A simple example will make the method clear:

Consider the case of a bundle of four units whose population parameters are $\frac{a}{b} = 0$, and V = 20%. From the above analysis:

$$h(t)_1 = Cf(t_1)\ (p_2 + p_3 + p_4)^3;\ \sum_{i=2}^{k} q_i \geq k-1;\ k=2,3,4 \quad \text{-------- I-9}$$

Assume that the first unit breaks at $t_1 = -2.0$. Then in order that the second break shall not occur at a higher total bundle load:

$$n\ g(t_1) \geq (n-1)\ g(t_2) \text{ or } 4\ g(t_1) \geq 3g(t_2)$$

The curves 4g(t), 3g(t), and 2g(t), are shown in Figure (22). Since $\frac{a}{b} = 0$, the plots are straight lines passing through the origin, and the load per unit can be expressed as a fraction of mean load as:

$$g(t) = \frac{Vt}{100} + 1 = \frac{t}{5} + 1$$

Thus for $t_1 = -2.0$, $g(t_1) = \frac{-2}{5} + 1 = 0.6$; $ng(t_1) = 4(0.6) = 2.40$. This condition is shown at point A in Figure (22). When the first unit breaks the load drops to B on the 3g(t) curve and builds up along it until the second unit breaks. To satisfy the condition that a maximum be reached when the first unit breaks, it follows that the point C must be no higher than the point A or since $4g(t_1) = 3g(t_2)$ in the limit, $g(t_2) = \frac{4}{3}\ g(t_1) = \frac{4}{3}\ (0.6) = 0.8$. But $g(t) = \frac{t}{5} + 1$, so that $t_2 = 5g(t)-5 = 5(0.8)-5 = -1$.

Similarly, when the second unit breaks the load drops to the point D and rises along the 2g(t) curve. Here, $4g(t_1) = 2g(t_3)$ or, $g(t_3) = \frac{4}{2}\ (0.6) = 1.2$ and thus $t_3 = 5(1.2)-5 = 1.0$.

For t_4 (not illustrated):

$$g(t_4) = \frac{4}{1}\ (0.6) = 2.4$$

$$t_4 = 5(2.4)-5 = 7$$

In Figure (23) is shown a normal frequency distribution corresponding to the values just calculated. By definition p_2 is the probability that any unit from the population has a breaking elongation lying between t_1 and t_2. Since $t_1 = -2.0$ and $t_2 = -1.0$, this is represented by the shaded area between these two points under the distribution curve. Similarly the shaded area from $t = -1.0$ to $t = +1.0$ represents p_3, and that from 1.0 to 7.0, p_4.

These p's must now be substituted into the expression for $h(t)_1$, Equations I-4. The expansion of Equations I-4 yield:

FIGURE 22
ILLUSTRATION OF SUCCESSIVE RUPTURES FOR LIMITING CONDITION FOR MAXIMUM BUNDLE LOADS

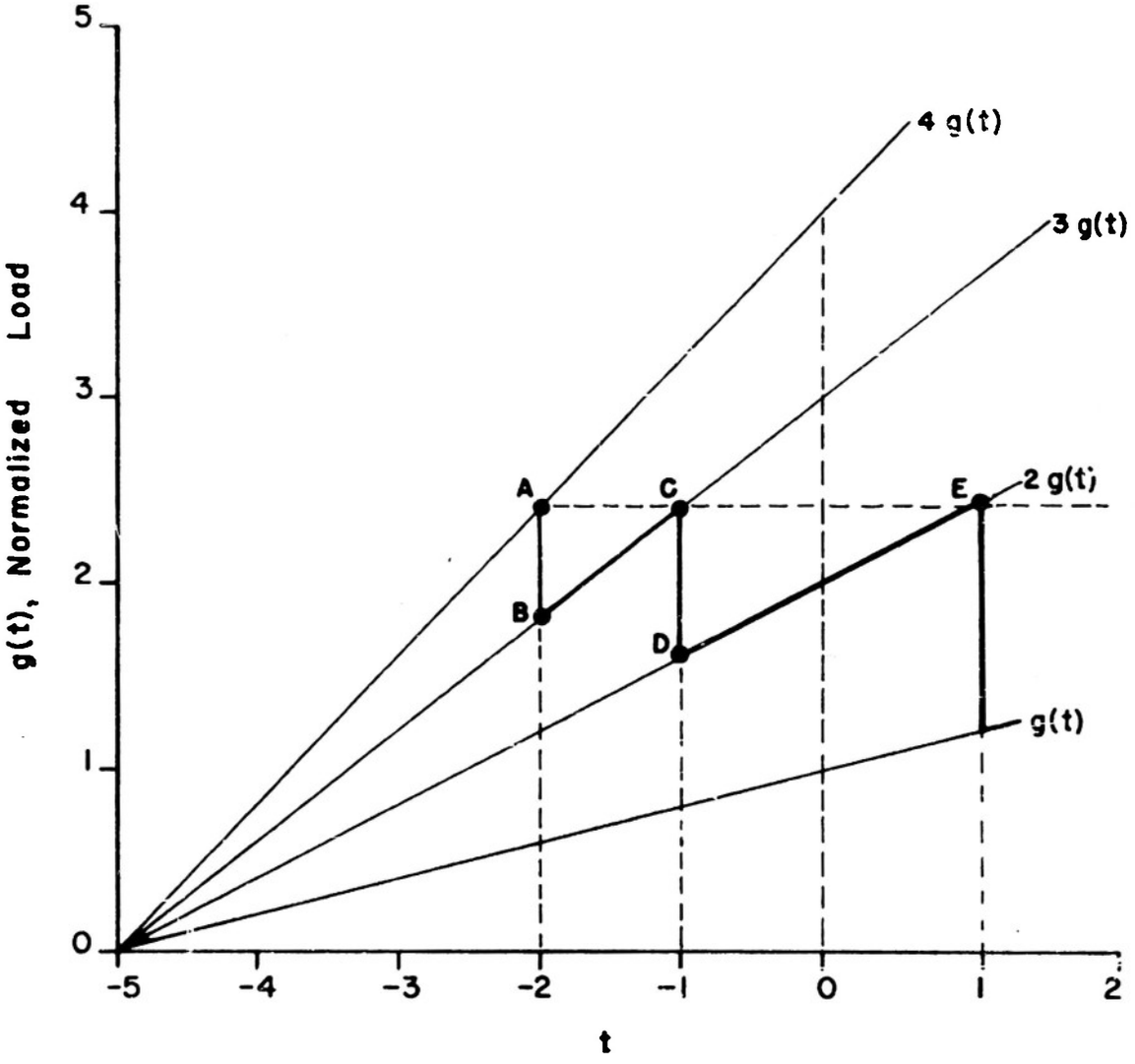

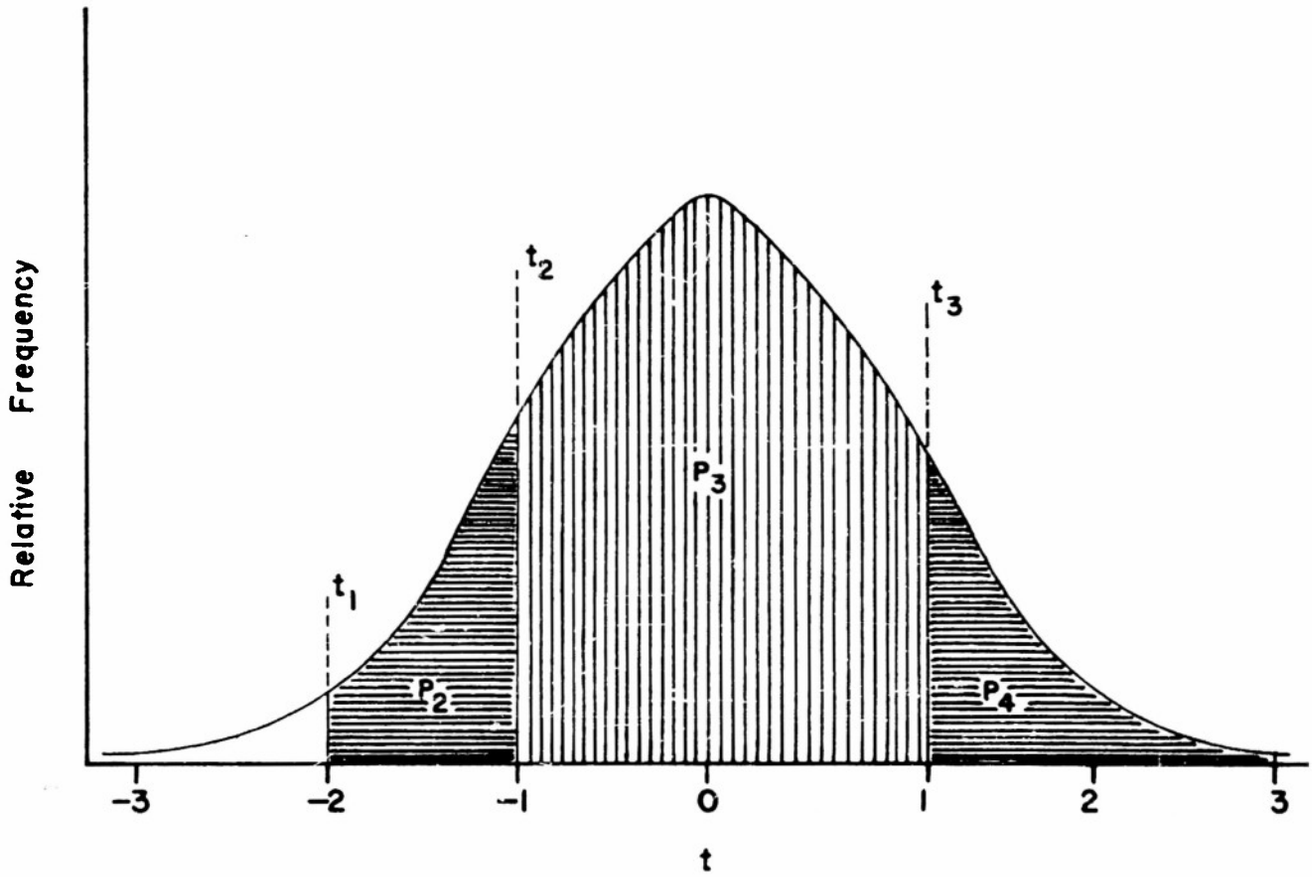

FIGURE 23

ILLUSTRATION OF P_i FOR $n = 4$, $V = 20\%$, $a/b = 0$

$$h(t)_1 = Cf(t_1)\left[p_2^3+p_3^3+p_4^3+3p_2^2p_3+3p_2^2p_4+3p_3^2p_2+3p_3^2p_4+3p_4^2p_2+3p_4^2p_3+6p_2p_3p_4\right]$$

$$\sum_{i=2}^{k} q_i \geq k-1;\ k = 2,3,4 \qquad \text{---I-10}$$

Each term of the expression must be examined, and if it does not fulfill the conditions specified in the second of Equations I-10, it must be rejected. This process eliminates all terms which are representative of cases where a maximum value of load is not reached when the first unit breaks. The following table illustrates the method:

				VALUES OF $\sum q_i$ FOR:				
TERMS	q_2	q_3	q_4	k = 2	k = 3	k = 4	ACCEPT	REJECT
p_2^3	3	0	0	3	3	3	✓	
p_3^3	0	3	0	(0)	3	3		✓
p_4^3	0	0	3	(0)	(0)	3		✓
$3p_2^2p_3$	2	1	0	2	3	3	✓	
$3p_2^2p_4$	2	0	1	2	2	3	✓	
$3p_3^2p_2$	1	2	0	1	3	3	✓	
$3p_3^2p_4$	0	2	1	(0)	2	3		✓
$3p_4^2p_2$	1	0	2	1	(1)	3		✓
$3p_4^2p_3$	0	1	2	(0)	(1)	3		✓
$6p_2p_3p_4$	1	1	1	1	2	3	✓	
Conditions for Acceptance				$\sum q_i \geq 1$	$\sum q_i \geq 2$	$\sum q_i \geq 3$		

A single circled value in any row is sufficient for rejection. Thus the first term, p_2^3, is acceptable. It represents the case where all three remaining units break in the region between t_1 and t_2. The second term p_3^3 is not acceptable. It represents the case where no breaks occur between t_1 and t_2 with three breaks between t_2 and t_3. This violates the condition that at least one must rupture between t_1 and t_2 in order that the load at t_1 be a maximum. The other terms can be handled in a similar manner. In each case the value of $\sum q_i$ in the k column must satisfy the value given at the bottom of the column in order to conform to the restrictions imposed by the requirement of a maximum bundle load at first unit break.

In the k = 4 column, the restriction imposed is that $\sum_{i=2}^{4} q_i \geq 3$. Clearly, $\sum_{i=2}^{4} q_i$ is always exactly 3 in this example, but the form of the table

is more general and can be used for cases where the total number of units is in excess of 4. Thus if n were 6, it would hardly be anticipated that there would be any appreciable number of bundle breaks which would have a maximum value when the fifth or sixth units broke. In this case, there would be no need to include the columns pertaining to t5 and t6, and the restrictions already shown in the table would apply.

The terms remaining in the n = 4 case which satisfy the conditions of maximum bundle load occurring at first unit break are:

$$p_2^3+3p_2^2p_3+3p_2^2p_4+3p_2p_3^2+6p_2p_3p_4$$

For computational purposes this is most conveniently written as:

$$(p_2+p_3+p_4)^3 - (p_3+p_4)^3 - 3p_2p_4^2$$

All necessary numbers can now be found from a table listing areas under the normal distribution curve, and ordinates to the curve. For this example where $t_1 = -2.0$, $t_2 = -1.0$, $t_3 = 1.0$, and $t_4 = 7$, the tables yield:

$$f(-2\ 0) = 0.05399$$

$$p_2 = \frac{1}{\sqrt{2\pi}}\int_{-2.0}^{-1.0} e^{\frac{-t^2}{2}}\,dt = 0.1359$$

$$p_3 = \frac{1}{\sqrt{2\pi}}\int_{-1.0}^{1.0} e^{\frac{-t^2}{2}}\,dt = 0.6827$$

$$p_4 = \frac{1}{\sqrt{2\pi}}\int_{1.0}^{7.0} e^{\frac{-t^2}{2}}\,dt = 0.1587$$

and thus:

$$h(-2.0)_1 = C(0.05399)\left[(0.1359+0.6827+0.1587)^3-(0.6827+0.1587)^3-3(0.1359)(0.1587)^2\right] = 1.769(10^{-2})C$$

In a like manner values of t_1 of -2.5, -1.5, -1.0, -0.5, 0.00, 0.5, and 1.0 were employed. The resulting curve is plotted in Figure (24), which is identical with Figure (9) of the text and is repeated here for ease of reference.

Next the case of a maximum at second unit break must be treated. Here:

$$h(t)_2 = Cf(t_2)\ (p_1+p_3+p_4)^3;\ \sum_{i=3}^{k} q_i = k-2,\ k=3,\ 4;\ q_1=1 \quad \text{----------I-11}$$

A chart similar to the one used for the previous case appears on Page xiii.

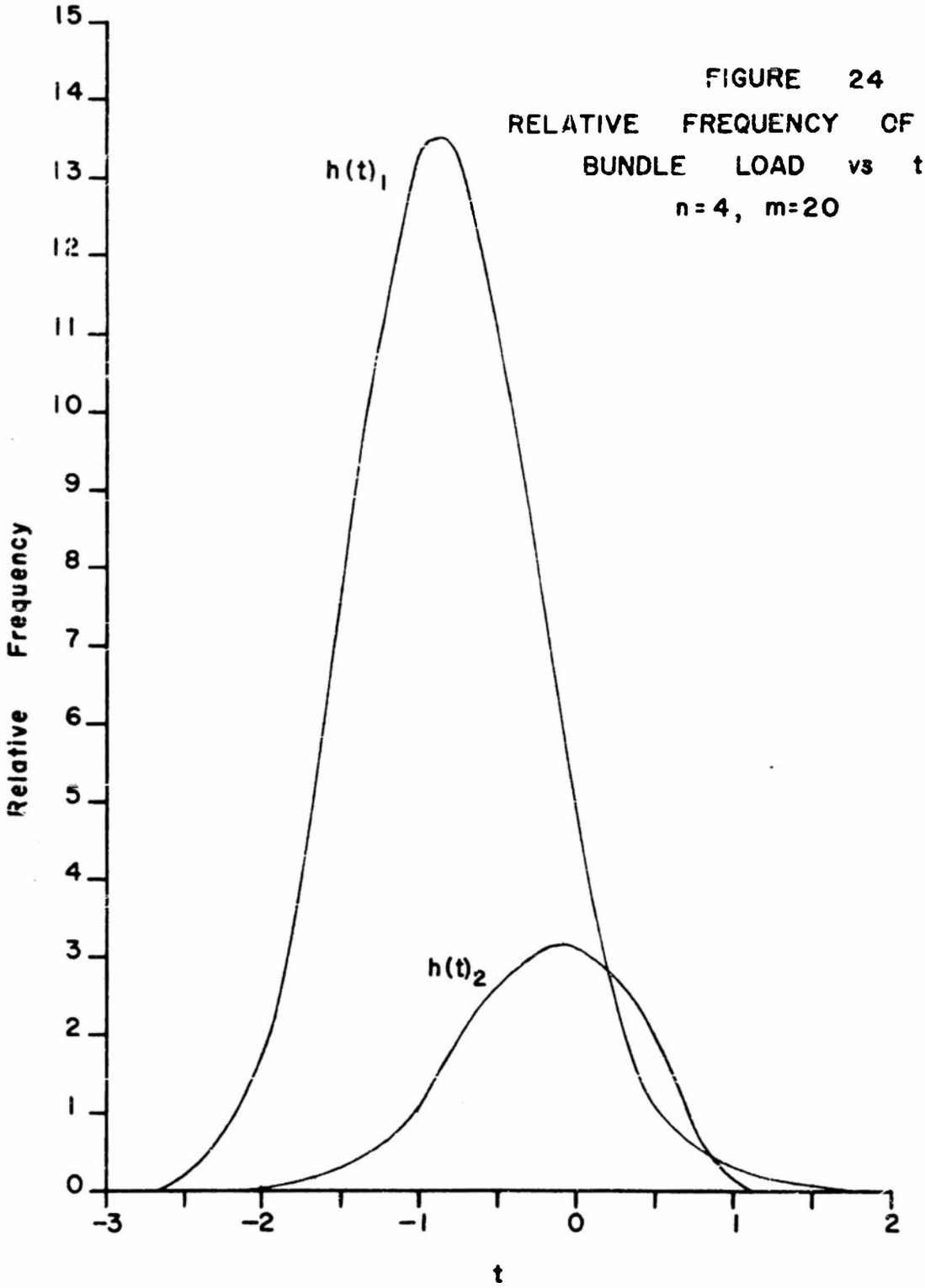

FIGURE 24
RELATIVE FREQUENCY OF MAXIMUM BUNDLE LOAD vs t
n = 4, m = 20

TERMS	q_1	q_3	q_4	VALUES OF $\sum q_i$ FOR: q_1	$k = 3$	$k = 4$	ACCEPT	REJECT
p_1^3	3	0	0	(3)	(0)	(0)		✓
p_3^3	0	3	0	(0)	3	3		✓
p_4^3	0	0	3	(0)	(0)	3		✓
$3p_1^2p_3$	2	1	0	(2)	1	(1)		✓
$3p_1^2p_4$	2	0	1	(2)	(0)	(1)		✓
$3p_1p_3^2$	1	2	0	1	2	2	✓	
$3p_1p_4^2$	1	0	2	1	(0)	2		✓
$3p_3^2p_4$	0	2	1	(0)	2	3		✓
$3p_3p_4^2$	0	1	2	(0)	1	3		✓
$6p_1p_3p_4$	1	1	1	1	1	2	✓	
Conditions for Acceptance				$q_1 = 1$	$\sum q_i \geq 1$	$\sum q_i \geq 2$		

A single circled value in any row is sufficient for rejection.

Clearly, the requirements are more stringent here than in the case of first unit rupture and only the terms $3p_1p_3^2$ and $6p_1p_3p_4$ remain. Then:

$$h(t)_2 = Cf(t_2)\ (3p_1p_3^2+6p_1p_3p_4)$$

This curve, $h(t)_2$, is plotted in Figure (24) together with $h(t)_1$. For the case of a maximum being reached where the third unit breaks, a similar table is made and it is found that only the $3p_1^2p_4$ and $6p_1p_2p_4$ terms remain, so that:

$$h(t)_3 = Cf(t_3)\ (3p_1^2p_4+6p_1p_2p_4)$$

The values obtained from this expression are so small compared to those from $h(t)_1$ and $h(t)_2$ that the $h(t)_3$ curve is neglected. Obviously $h(t)_4$ will also be insignificant and thus only the $h(t)_1$ and $h(t)_2$ curves need be averaged.

Once the $h(t)_i$ curves have been plotted, the ordinate scale is no longer of any significance since only the average abscissa value is required when the $h(t)_i$ curves are symmetrical. The process is now very simple. The $h(t)_1$ curve has a mean elongation occurring at $t = -0.84$, as determined by inspection, and an enclosed area of 24.52 units as determined by a planimeter. For the $h(t)_2$ curve, the corresponding figures are -0.13 and 5.93 respectively. Since, in the example the elongation variability (coefficient of variation of

unit elongation to break) is 20%, and $\frac{a}{b}$ is zero, the abscissa can be expressed as per cent of mean unit rupture load per unit. Thus for the $h(t)_1$ curve the result is:

$$g(\bar{t}_1) = 100 - 0.84\ (20) = 83.2$$

and for the $h(t)_2$ curve:

$$g(\bar{t}_2) = 100 - 0.13\ (20) = 97.4$$

In the first case all four units are intact when the maximum bundle load occurs, but in the second case only three units are intact. Then the efficiency of translation which is the average bundle load expressed as a per cent of the mean unit rupture load is:

$$\frac{4\ (83.2)\ (24.52) + 3(97.4)\ (5.93)}{4(24.52 + 5.93)} = 81.2\%$$

APPENDIX II

Analysis of Strength of Bundle When First Unit Breaks

In Appendix I the case of maximum bundle strength was analyzed. For many purposes, a structure may be considered to have failed when the first element has ruptured. If there are a small number of units in the group, and the mechanical interaction between units is large, then it is possible that the elastic recovery of those portions of the broken unit to either side of the break can stress the remaining unbroken units, and in some cases break them. This "snap-back" effect can be of significance when the total number of units is small and the coefficient of variation of elongation to break of the units is small. In a practical sense, there is no difficulty in predictability since under the conditions of maximum effect of "snap-back", there is only a very small difference between average bundle load at first unit break and average maximum bundle load. This does not however, deny the very practical fact in many cases the mechanical utility of the structure is destroyed as soon as the first unit breaks, and thus it is of significance to consider the analysis of the problem. The method for finding the average load supported by a bundle of parallel units when the first unit breaks will now be developed.

Consider a population of units with a mean breaking elongation e_m, a normal distribution of elongations to break with a coefficient of variation of elongation to break V. Now define the following quantities:

p = probability of any unit breaking at an elongation in excess of $t = \frac{1}{\sqrt{2\pi}} \int_t^{\infty} f(t)\, dt$

f(t) = relative frequency of break at t (ordinate to normal curve).

h = relative frequency of first unit break at elongation t.

If a bundle of n parallel units is stressed to a given elongation t, then the probability of having (n-1) units intact at this point will be the probability of having any given individual unit intact taken to the (n-1) power, or $(p)^{n-1}$. The additional restriction, that the first unit shall have just ruptured, is satisfied by multiplying this quantity by f, the relative frequency of break at t. A normalizing constant, described in Appendix I, has been omitted here since it was shown there that it has no effect on the mean. A curve can now be plotted of h, the relative frequency of a first unit break, versus t, where:

$$h = f(t)p^{n-1} \qquad \text{II-1}$$

By assuming various values for t and determining for each such value the corresponding value of p, it is possible to evaluate Equation II-1 for all bundle sizes, i.e., all values of n.

The results for values of n from 1 to 15 are plotted in Figure (7). The mean value of t for each of these curves is plotted versus n in Figure (8). This mean value can be interpreted as an efficiency using a linear approximation to the stress-strain curve. That is, one need only find the load on the linear curve corresponding to the t value found and divide this by the mean breaking load. Using the parameter m as previously described, curves of efficiency versus bundle size for m = 10, 20, and 30 have been plotted in Figure (25). These curves also appear in Figure (10) of the text.

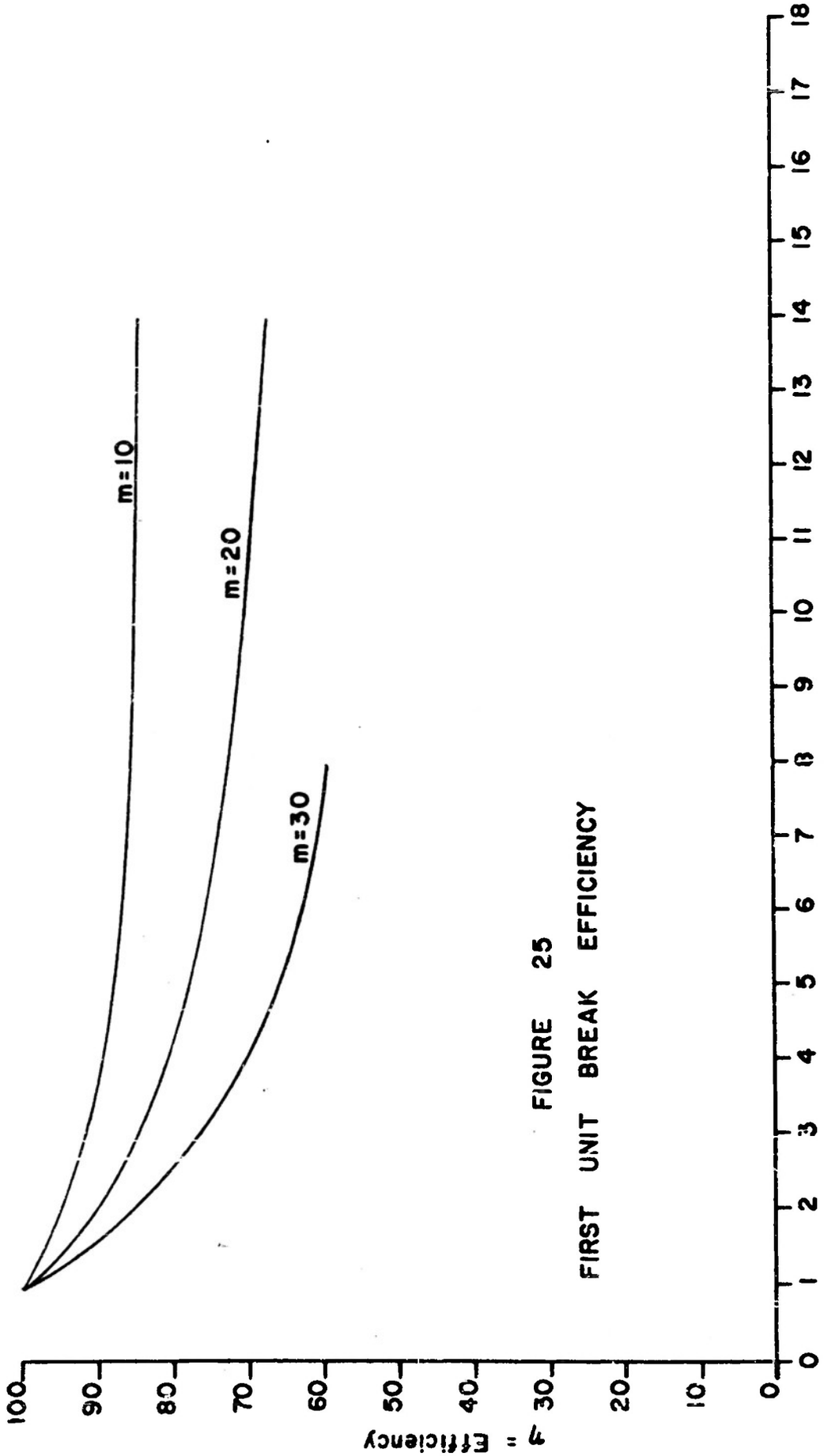

FIGURE 25

FIRST UNIT BREAK EFFICIENCY

APPENDIX III

Analysis of Seven Ply Yarn Strength

From the definition of a parallel bundle given at the beginning of Appendix I, it is clear that a seven ply yarn cannot be considered as such a group. In two or three ply yarns of uniform geometry, the yarn strain is the same in all yarns, by symmetry. The idealized seven ply yarn (see below) although rotationally symmetric, is not radially symmetric, and thus all of the singles yarns cannot be considered as equally strained. The presence of the core in a seven ply yarn creates the difference between this structure and a parallel bundle.

The analysis of seven ply yarn strength however, is similar to that of the parallel bundle strength, the only differences arising as a result of the variation in strain between the core and the external units.

The idealized geometry for the seven ply yarn consists of a circular core of radius R_y surrounded by six circular units with the same radius as illustrated in Figure (26).

If the external units are inclined to the core at an angle θ_p, then their strain in terms of the plied yarn strain, e_p, will be $e_p\cos^2\theta_p$ (see 3) and the load on the external yarns will be that corresponding to this strain as given by the stress-strain curve of the singles yarns. Thus, if a linear approximation to the shape of the singles yarn stress-strain curve is used here as before, the tension in the core will be $(a+be_p)$, and in each of the outside yarns, $(a+be_p\cos^2\theta_p)$. For purposes of statistical calculation all quantities must, as previously, be expressed in terms of t.

Let primed letters refer to the external singles yarns and unprimed letters to the core yarn. Then:

$$e = e_p;\ e' = e_p\cos^2\theta_p \qquad \text{III-1}$$

By definition:

$$t = \frac{e - e_m}{\sigma} \qquad \text{III-2}$$

and thus:

$$t' = \frac{e'-e_m}{\sigma} = \frac{e\cos^2\theta_p - e_m}{\sigma} = \frac{e-e_m-e+e\cos^2\theta_p}{\sigma} = t - \frac{e(1-\cos^2\theta_p)}{\sigma} = t-\frac{e\sin^2\theta_p}{\sigma}$$

$$\text{III-3}$$

But since $\sigma = \frac{e_m V}{100}$:

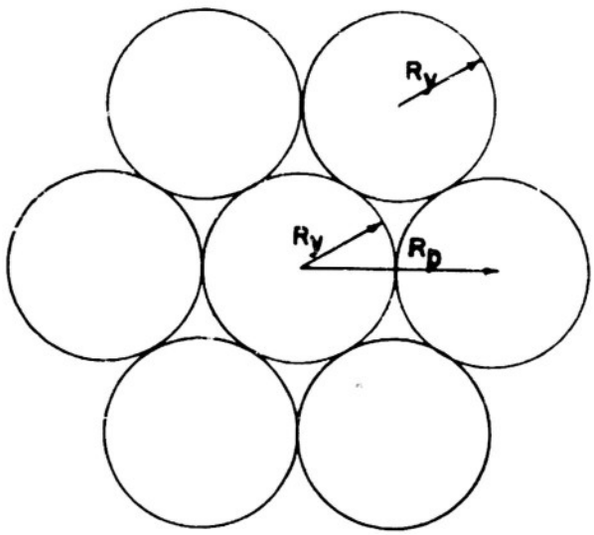

FIGURE 26

IDEALIZED 7-PLY YARN

$$t' = t - \frac{100\,e}{e_m V} \sin^2\theta_p \qquad \text{III-4}$$

Since:

$$t = \frac{e-e_m}{\sigma} = \frac{e-e_m}{e_m V}\,100;\quad e = \frac{te_m}{100} V + e_m = \frac{e_m}{100}(tV + 100) \qquad \text{III-5}$$

Therefore:

$$t' = t - \frac{e_m}{100}\,\frac{(tV + 100)}{e_m V} \sin^2\theta_p \times 100 \qquad \text{III-6}$$

or:

$$t' = t - (t + \frac{100}{V}) \sin^2\theta_p$$

The plied yarn load contributed by each of the external yarns is equal to the tension in each external yarn times the cosine of the ply helix angle. Thus, if the load-elongation diagram of the singles yarns is expressed as a function of t, g(t), the tension on the plied yarn when all units are intact is:

$$p = g(t) + 6\,g(t')\cos\theta_p \qquad \text{III-7}$$

Following an analysis very similar to that of Appendix I, a number of different breaking configurations are assumed, and the strength of each configuration together with the probability of such a configuration not attaining a higher strength is calculated.

For example: Let the core yarn break at an elongation t_1, with all external yarns intact. The strength of the configuration at this point will be $g(t_1) + 6g(t'_1)\cos\theta_p$. In order that no subsequent load shall be greater than this it follows, in the limit, that:

$$g(t_1) + 6g(t'_1)\cos\theta_p = 6g(t_2')\cos\theta_p = 5g(t_3')\cos\theta_p = 4g(t_4')\cos\theta_p \text{ etc.}$$

$$\text{III-8}$$

where t_2' is the point at which the first external yarn ruptures, t_3' when the second rupture, etc. The probability of such a configuration, using the nomenclature of Appendix I, is:

$$Cf(t_1)\,(p_2'+p_3'\ldots+p_7')^6, \sum_{i=2}^{k} q_i \geq k-1,\ k=2,3\ldots\ldots7 \qquad \text{III-9}$$

By using different values of t and assuming different breaking configurations, sets of curves similar to those given in Appendix I can be plotted and averaged.

For example, another configuration to be assumed is that for which maximum load takes place when the first unit breaks, and the first unit is not the core but instead one of the external yarns, with the second unit which ruptures being either the core yarn or one of the five remaining external yarns. Thus this case is not a single configuration. In the computations, a sufficient number of configurations were analyzed to yield results of engineering accuracy. The plotting and averaging procedure is very similar to that described in Appendix I, and will not be repeated here. The only difference is that in weighting the contributions to maximum bundle strength of each configuration, the weighting factor is dependent not only upon how many units are intact, but also upon whether these remaining yarns are core or external units, i.e., the $\cos\theta_p$ of the external yarns must be included.

The results, for several cases, are plotted in Figure (11) of the text.

ACKNOWLEDGEMENT

The authors wish to acknowledge the assistance of Mr. David Himmelfarb of the Boston Naval Shipyard both for supplying the various strands and ropes studied in this work and also for his very valuable suggestions and discussions on strand and rope performance. The labors of Mrs. M. Teixeira and Miss J. Rea in making the numerous tests and calculations are gratefully noted. The work has benefited from numerous discussions with Professor S. Backer of the Massachusetts Institute of Technology. Acknowledgement is also made to Professor E. R. Schwarz of the Textile Division, Massachusetts Institute of Technology, for permission to use the thesis of T. Chow for geometric analysis comparisons.

BIBLIOGRAPHY

1. Platt, M. M., Klein, W. G., and Hamburger, W. J., Factors Affecting the Translation of Certain Mechanical Properties of Cordage Fibers Into Cordage Yarns, Technical Report Number 6 to the Office of Naval Research, Contract Number N7 ONR 421, Task Order I, 1 January, 1952.

2. Platt, M. M., Klein, W. G., and Hamburger, W. J., Mechanics of Elastic Performance of Textile Materials, Part IX, Textile Research Journal, 1952, 22, October.

3. Platt, M. M., Mechanics of Elastic Performance of Textile Materials, Part III, Ibid, 1950, 20, January.

4. Schwartz, E. R., Twist Structure of Plied Yarns, Textile Research Journal, 1950, 20, March.

5. Chow, T., Unpublished Master's Thesis, Massachusetts Institute of Technology, Textile Division, June, 1948.

6. Platt, M. M., Klein, W. G., and Hamburger, W. J., Mechanics of Elastic Performance of Textile Materials, Supplement to Part IX, Textile Research Journal, 1952, 22, December.

DISTRIBUTION LIST

Chief of Naval Research
Department of the Navy
Washington 25, D. C.
Attn: Code 424 (2)

Director
Office of Naval Research
Branch Office
150 Causeway Street
Boston, Massachusetts (1)

Director
Office of Naval Research
Branch Office
346 Broadway
New York 13, New York (1)

Director
Office of Naval Research
Branch Office
Tenth Floor
The John Crerar Library Building
86 East Randolph Street
Chicago 1, Illinois (1)

Director
Office of Naval Research
Branch Office
1000 Geary Street
San Francisco 9, California (1)

Director
Office of Naval Research
Branch Office
1030 E. Green Street
Pasadena, California (1)

Officer-in-Charge
Office of Naval Research
Navy #100
Fleet Post Office
New York, New York (2)

Director
Naval Research Laboratory
Washington 25, D. C.
Attn: Technical Information
Officer (6)

Armed Services Technical Information
Document Service Center
Knott Building
Dayton 2, Ohio (5)

Office of Technical Services
Department of Commerce
Washington 25, D. C. (1)

Chief, Bureau of Ships
Department of the Navy
Washington 25, D. C.
Attn: G. I. Dewey, Code 354 (1)

Office of Quartermaster General
Department of the Army
Washington 25, D. C.
Attn: Research & Development Division

National Advisory Committee
for Aeronautics
1724 F. Street, N. W.
Washington 25, D. C. (1)

Quartermaster Research & Development
Laboratories
Philadelphia Quartermaster Depot
2800 South 20th Street
Philadelphia 45, Pennsylvania
Attn: Chief, Textile Research
Laboratory (1)

Textile Research Journal
10 East 40th Street
New York 16, New York
Attn: Mr. Julian Jacobs (1)

DISTRIBUTION LIST (continuation)

Development Department
Naval Clothing Depot
29th Street and 3rd Avenue
Brooklyn 32, New York (1)

Director
National Bureau of Standards
Washington 25, D. C.
Attn: Chief, Organic & Fibrous
Division (1)

Commanding General
Wright-Air Development Center
Wright-Patterson Air Force Base
Ohio
Attn: Materials Laboratory (1)

Whitlock Cordage Company
Foot of Lafayette Street
Jersey City, New Jersey
Attn: Mr. William Whitlock III (1)

Textile Research Institute
Princeton, New Jersey (1)

North Carolina State College
School of Textiles
Raleigh, North Carolina (1)

Clemson Agricultural College
School of Textiles
Clemson, South Carolina (1)

Director
U. S. Department of Agriculture
Eastern Regional Laboratory
Philadelphia 18, Pa. (1)

Director
Lowell Textile Institute
Lowell, Massachusetts (1)

Columbian Rope Company
Auburn, New York
Attn: Mr. Raymond Starr (1)

U.S. Department of Agriculture
Plant Industry Station
Beltsville, Maryland
Attn: Dr. Brittain Robinson (3)

Raymond E. Miskelly, Research Director
Plymouth Cordage Company
North Plymouth, Massachusetts (1)

New Bedford Cordage Company
New Bedford, Massachusetts
Attn: Mr. Martin Walter, Jr. (1)

U. S. Department of Agriculture
Southern Regional Research Laboratory
New Orleans 19, Louisiana (1)

Chief, Bureau of Supplies and Accounts
Research & Development Division
Clothing
Washington 25, D. C. (2)

National Research Council
Ottawa, Canada
Attn: Dr. P Larose (1)

Mr. E. Howard Hutchinson
Newport Industries
80 Federal Street
Boston, Massachusetts (1)

Library
U.S. Department of Agriculture
Washington 25, D. C. (1)

Dr. Carleton G. Lutts
Boston Naval Shipyard
Charlestown, Massachusetts (1)

Mr. David Himmelfarb
Boston Naval Shipyard
Charlestown, Massachusetts (1)